

# Temperature Dependence of the Masses of Various Meson States: A Comparative Study in SU(3) and SU(4) extended Linear-Sigma Model

Alexandra Friesen<sup>1</sup>, Yu. Kalinovsky<sup>1</sup>, Norhan M. Rfeek<sup>2</sup>, Azzah A. Alshehri<sup>3</sup>, Abdel Nasser Tawfik<sup>4,5\*</sup>

<sup>1</sup>*Joint Institute for Nuclear Research (JINR), 141980 Dubna, Russia Federation*

<sup>2</sup>*Assiut University, Faculty of Science, Physics Department, 71515 Assiut, Egypt*

<sup>3</sup>*University of Hafr Al Batin (UHB), University College at Nairiyah, Department of Science and Technology, Nairiyah 31981, Saudi Arabia*

<sup>4</sup>*Islamic University, Physics Department, 42351 Madinah, Saudi Arabia and*

<sup>5</sup>*Ahram Canadian University (ACU), Faculty of Engineering, 12556 Giza, Egypt*

In the extended Linear-Sigma Model (eLSM), the chiral phase structure of meson states, including pseudoscalars ( $J^{pc} = 0^{-+}$ ), scalars ( $J^{pc} = 0^{++}$ ), vectors ( $J^{pc} = 1^{--}$ ), and axial-vectors ( $J^{pc} = 1^{++}$ ), is investigated with the mean-field approximation. A systematic comparison between SU(3) and SU(4) configurations is provided. It has been found that the estimations of meson masses derived from SU(4) eLSM are more congruent with experimental values than those derived from SU(3) eLSM. Consequently, we conclude that an increase in quark degrees of freedom significantly enhances the accuracy of meson mass simulations. We investigate the effect of temperature on the masses of various meson states calculated in the SU(3) and SU(4) eLSM. After establishing all the fitting parameters, the temperature dependence of meson masses shows that although various meson states exhibit unique patterns in their mass changes with temperature, they all seem to share a similar range of dissolution temperatures. This means that the critical temperature that marks the phase transition from hadrons to quarks appears to vary slightly depending on the meson states. In this regard, we find that the quarkonium states, formed by a quark and its antiquark, are largely unaffected by variations in the temperature.

## I. Introduction

To analyze different properties of QCD, several low-energy effective QCD-like models have been established, thereby providing insights into the phase structure at finite temperatures, densities, and in the presence of magnetic and electric fields [1–4]. In the limit of vanishing quark masses,

---

\* a.tawfik@fue.edu.eg

chiral symmetry emerges as a fundamental symmetry in QCD [5–8]. On the other hand, in the limit of finite quark masses, chiral symmetry becomes spontaneously broken. In this limit, the chiral condensate represents the associated order parameter. With small quark masses, the explicit breaking of chiral symmetry for the up and down quarks [9] causes the pseudo-Goldstone bosons to acquire finite masses, such as the light pseudoscalar mesons, which include pions [10, 11]. For heavier quark flavors, including strange and charm quarks, the explicit breaking intensifies, resulting in the emergence of both hidden and open charmed mesons like  $D$  [12] and  $\chi_{c0}$  meson [13], respectively. Under extreme conditions of high temperature and/or density, the in-medium chiral condensate seems to vanish, demonstrating the restoration of chiral symmetry and the emerging of meson state degeneracy [14, 15].

The QCD phase structure can be explored using low-energy QCD methods, such as Dyson–Schwinger equations [16–18] and chiral perturbation theory [19], etc. Different statistical thermal models are also employed in examining QCD phase structure. This includes, for instance the Hadron Resonance Gas (HRG) [20, 21] Nambu–Jona–Lasinio (NJL) [22, 23], and Linear–Sigma Model (LSM) [3, 24, 25]. In effective QCD-like models, such as LSM [3, 24, 25], pion mesons can be contracted with two quark flavors, specifically in an  $SU(2)$  configuration [26–28]. This framework also facilitates a systematic examination of light quark condensates [29]. The  $SU(3)$  configuration enables the construction of nonet meson masses [3, 25], the study of the QCD phase transition [30, 31], and the investigation of strange condensate [1, 3]. The  $SU(4)$  configuration evidently incorporates the charm quark, allowing for the analysis of the corresponding condensate. A systematic investigation of charmed meson masses was analytically derived and presented in Ref. [32]. This manuscript is devoted to exploring the in-medium modifications of various charmed meson masses. A systematic analysis comparing the temperature dependence of various meson masses of  $SU(3)$  and  $SU(4)$  is also conducted.

Recent advancements in experimental high-energy particle physics, particularly at the Large Hadron Collider (LHC) at CERN and the Relativistic Heavy Ion Collider (RHIC) at Brookhaven National Laboratory (BNL), especially the Beam Energy Scan program of the STAR experiment [33], have brought considerable prominence among researchers to the in-medium modifications of various hadron states [34–36]. The analysis of in-medium modifications of various hadron properties is anticipated in future facilities including the Facility for Antiproton and Ion Research (FAIR), at GSI, Darmstadt-Germany [37–39] and Nuclotron-based Ion Collider fAcility (NICA) at JINR, Dubna-Russia [40].

In-medium modifications of charmed mesons are particularly interesting because they serve as

probes for the hot and dense medium created during heavy-ion collisions. However, modeling the charm sector using effective models like the eLSM comes with its own set of challenges, especially due to the necessity of an extra mass term  $-2Tr[\epsilon\Phi^\dagger\Phi]$  [41], along with the complex interactions between light and heavy flavor condensates. While the SU(3) eLSM has proven effective in exploring light meson states and their chiral phase structure [24, 25], there is still a gap when it comes to a systematic, comparative analysis of meson masses in SU(4) configurations. In this work, we aim to provide a detailed examination of how various meson states - pseudoscalars, scalars, vectors, and axial-vectors - depend on temperature, all within the eLSM framework for both SU(3) and SU(4) flavor symmetries. We adopt the mean-field approximation and include finite-temperature effects using the grand potential, which accounts for contributions from quark-antiquark pairs and the Polyakov loop. Our investigation examines the significance of the  $U(1)_A$  anomaly (denoted by a constant  $c$ ) in different symmetry configurations, and we compare the pseudo-critical temperatures that mark the restoration of chiral symmetry.

This manuscript is structured as follows. In Section II, the extended Linear Sigma Model (eLSM) is reviewed. The configurations for SU(3) and SU(4) are discussed in Sections II A and II B, respectively. Section II C provides a detailed explanation of the finite temperature formalism for the masses of various meson states. The parametrization along with the numerical results is examined in Section III. The final conclusions are presented in Section IV.

## II. Extended Linear Sigma Model

The LSM [42–47] provides a remarkably accurate description of various meson states [24, 25, 32]. As the degrees of freedom related to the quark flavors  $N_f$ , increase, so does the number of meson states that can be created. The SU(3) meson states were derived and introduced in Refs. [24, 25]. The analytical derivation of SU(4) meson states is introduced in Refs. [32, 48].

The Lagrangian for the mesonic sector, which contains scalar, pseudoscalar, vector, and axial-vector mesons, together with their interactions and anomalies, is built as follows [32]:

$$\mathcal{L} = \mathcal{L}_{SP} + \mathcal{L}_{VA} + \mathcal{L}_{Int} + \mathcal{L}_{U(1)_A}, \quad (1)$$

$$\mathcal{L}_{SP} = \text{Tr} \left[ (D^\mu \Phi)^\dagger (D^\mu \Phi) - m^2 \Phi^\dagger \Phi \right] - \lambda_1 [\text{Tr}(\Phi^\dagger \Phi)]^2 - \lambda_2 \text{Tr}(\Phi^\dagger \Phi)^2 + \text{Tr}[H(\Phi + \Phi^\dagger)], \quad (2)$$

$$\begin{aligned} \mathcal{L}_{AV} = & -\frac{1}{4} \text{Tr}(L_{\mu\nu}^2 + R_{\mu\nu}^2) + \text{Tr} \left[ \left( \frac{m_1^2}{2} + \Delta \right) (L_\mu^2 + R_\mu^2) \right] \\ & + i \frac{g_2}{2} (\text{Tr}\{L_{\mu\nu}[L^\mu, L^\nu]\} + \text{Tr}\{R_{\mu\nu}[R^\mu, R^\nu]\}) \\ & + g_3 [\text{Tr}(L_\mu L_\nu L^\mu L^\nu) + \text{Tr}(R_\mu R_\nu R^\mu R^\nu)] + g_4 [\text{Tr}(L_\mu L^\mu L_\nu L^\nu) + \text{Tr}(R_\mu R^\mu R_\nu R^\nu)] \\ & + g_5 \text{Tr}(L_\mu L^\mu) \text{Tr}(R_\nu R^\nu) + g_6 [\text{Tr}(L_\mu L^\mu) \text{Tr}(L_\nu L^\nu) + \text{Tr}(R_\mu R^\mu) \text{Tr}(R_\nu R^\nu)], \end{aligned} \quad (3)$$

$$\mathcal{L}_{Int} = \frac{h_1}{2} \text{Tr}(\Phi^\dagger \Phi) \text{Tr}(L_\mu^2 + R_\mu^2) + h_2 \text{Tr}[|L_\mu \Phi|^2 + |\Phi R_\mu|^2] + 2h_3 \text{Tr}(L_\mu \Phi R^\mu \Phi^\dagger), \quad (4)$$

$$\mathcal{L}_{U(1)_A} = c[\text{Det}(\Phi) + \text{Det}(\Phi^\dagger)] + c_0[\text{Det}(\Phi) - \text{Det}(\Phi^\dagger)]^2 + c_1[\text{Det}(\Phi) + \text{Det}(\Phi^\dagger)] \text{Tr}[\Phi \Phi^\dagger]. \quad (5)$$

The *complex* matrices for scalars  $\sigma_a$ , i.e.,  $J^{PC} = 0^{++}$ , pseudoscalars  $\pi_a$ , i.e.  $J^{PC} = 0^{-+}$ , vectors  $V_a^\mu$ , i.e.,  $J^{PC} = 1^{--}$  and axial-vectors  $A_a^\mu$ , i.e.,  $J^{PC} = 1^{++}$  meson states can be constructed as

$$\Phi = \sum_{a=0}^{N_f^2-1} T_a (\sigma_a + i\pi_a), \quad L^\mu = \sum_{a=0}^{N_f^2-1} T_a (V_a^\mu + A_a^\mu), \quad R^\mu = \sum_{a=0}^{N_f^2-1} T_a (V_a^\mu - A_a^\mu). \quad (6)$$

The various generators are defined according to the number of quark flavors  $N_f$ , while  $T_a$  are the corresponding generators of  $U(N_f)$  can be expressed as  $T_a = \hat{\lambda}_a/2$ , with  $a = 0 \dots (N_f^2 - 1)$  and  $\hat{\lambda}$  are the Gell–Mann matrices.

The covariant derivative

$$D^\mu \Phi \equiv \partial^\mu \Phi - i g_1 (L^\mu \Phi - \Phi R^\mu) - ie A^\mu [T_3, \Phi], \quad (7)$$

is to be associated with the degrees of freedom for (pseudo-)scalar and (axial-)vector and couples them through the coupling constant  $g_1$ .

$$L^{\mu\nu} \equiv \partial^\mu L^\nu - ie A^\mu [T_3, L^\nu] - \{\partial^\nu L^\mu - ie A^\nu [T_3, L^\mu]\}, \quad (8)$$

$$R^{\mu\nu} \equiv \partial^\mu R^\nu - ie A^\mu [T_3, R^\nu] - \{\partial^\nu R^\mu - ie A^\nu [T_3, R^\mu]\}, \quad (9)$$

where  $A^\mu = g A_\mu^a \lambda^a / 2$  is the electromagnetic field. The constant  $g$  is the Yukawa coupling, which is fixed from the non-strange constituent quark mass as  $g = 2m_q/\bar{\sigma}_x$ . The field  $\Phi$  is expressed as

$$\Phi = \sum_{a=0}^{N_f^2-1} T_a (\sigma_a + i\pi_a). \quad (10)$$

Expressions for  $T_a \sigma_a$  and  $T_a \pi_a$  can be found in Refs. [32, 48]. According to Refs. [32, 48], the global chiral invariance of the Lagrangian for  $N_f = 4$  is identical to that of  $N_f = 3$ . However, for  $N_f = 4$ , the mass term  $\mathcal{L}_{\text{emass}} = -2\text{Tr}[\epsilon \Phi^\dagger \Phi]$  must be included [41]. The origin of this term can be understood from the equivalence between the symmetry-breaking Hamiltonians of the  $SU(4) \times SU(4)$  and  $SU(3) \times SU(3)$  group [49, 50].

Starting with the SU(3) configuration of eLSM, the following section goes over the essential characteristics.

### A. SU(3) configuration

The tree-level mesonic potential for the scalar-pseudoscalar states is presented in the Appendix A, Eq. (A1). For the SU(3), this is reduced to

$$U(\sigma) = \frac{m^2}{2}\sigma_a^2 - \mathcal{G}_{abc}\sigma_c\sigma_a\sigma_b + \frac{1}{3}\mathcal{F}_{abcd}\sigma_a\sigma_b\sigma_c\sigma_d - h_a\sigma_a, \quad (11)$$

where the coefficients  $\mathcal{G}_{ab}$ ,  $\mathcal{G}_{abc}$ ,  $\mathcal{G}_{abcd}$ ,  $\mathcal{F}_{abcd}$ ,  $\mathcal{H}_{abcd}$  are detailed in the Appendix A.

It is more convenient to undertake the subsequent analysis in terms of the pure non-strange and strange fields, which are obtained respectively from the following transformation:

$$\begin{pmatrix} \sigma_x \\ \sigma_y \end{pmatrix} = \frac{1}{3} \begin{pmatrix} \sqrt{2} & 1 \\ 1 & -\sqrt{2} \end{pmatrix} \begin{pmatrix} \sigma_0 \\ \sigma_8 \end{pmatrix}. \quad (12)$$

The explicit chiral symmetry breaking parameters in the pseudo-scalar sector, i.e., the expression  $\text{Tr}[\mathcal{H}(\Phi + \Phi^\dagger)]$  in Eq. (1), allowing the transformation of  $h_0$  and  $h_8$  using the same transformation basis

$$H_{SU(3)} = T_0 h_0 + T_8 h_8 \equiv \frac{1}{2} \begin{pmatrix} h_x & 0 & 0 \\ 0 & h_x & 0 \\ 0 & 0 & \sqrt{2}h_y \end{pmatrix}. \quad (13)$$

Then the tree-level mesonic potential for the SU(3) configuration reads

$$\begin{aligned} U(\sigma_x, \sigma_y) = & \frac{m^2}{2}(\sigma_x^2 + \sigma_y^2) - \frac{c}{2\sqrt{2}}\sigma_x^2\sigma_y + \frac{\lambda_1}{2}\sigma_x^2\sigma_y^2 + \frac{1}{8}(2\lambda_1 + \lambda_2)\sigma_x^4 \\ & + \frac{1}{4}(\lambda_1 + \lambda_2)\sigma_y^4 - h_x\sigma_x - h_y\sigma_y. \end{aligned} \quad (14)$$

The global minimization of the grand potential determines the  $h_x$  and  $h_y$  as

$$h_x = m^2\sigma_x - \frac{c}{\sqrt{2}}\sigma_x\sigma_y - \lambda_1\sigma_x\sigma_y^2 + \frac{1}{2}(2\lambda_1 + \lambda_2)\sigma_x^3, \quad (15)$$

$$h_y = m^2\sigma_x - \frac{c}{2\sqrt{2}}\sigma_x^2 - \lambda_1\sigma_x^2\sigma_y + (\lambda_1 + \lambda_2)\sigma_y^3. \quad (16)$$

The tree-level masses of mesons are defined from the quadratic terms of the Lagrangian and are presented in detail in Appendix B.

The following section introduces the SU(4) configuration.

## B. SU(4) configuration

The tree-level mesonic potential for the scalar and pseudoscalar states in the SU(4) configuration can be derived from Eq. (A1)

$$U(\bar{\sigma}) = \frac{m^2}{2}\bar{\sigma}_a^2 + \frac{1}{3}[\mathcal{F}_{abcd} + \mathcal{G}_{abcd}]\bar{\sigma}_a\bar{\sigma}_b\bar{\sigma}_c\bar{\sigma}_d - h_a\bar{\sigma}_a + \epsilon_a\sigma_a^2. \quad (17)$$

The corresponding basis transformation to pure non-strange, strange, and charm fields, respectively, reads

$$\begin{pmatrix} \sigma_x \\ \sigma_y \\ \sigma_c \end{pmatrix} = \begin{pmatrix} \frac{1}{\sqrt{2}} & \frac{1}{\sqrt{3}} & \frac{1}{\sqrt{6}} \\ \frac{1}{2} & -\sqrt{\frac{2}{3}} & \frac{1}{2\sqrt{3}} \\ \frac{1}{2} & 0 & -\frac{\sqrt{3}}{2} \end{pmatrix} \begin{pmatrix} \sigma_0 \\ \sigma_8 \\ \sigma_{15} \end{pmatrix}. \quad (18)$$

The explicit chiral symmetry breaking parameters allow for the transformation of  $h_0$ ,  $h_8$ , and  $h_{15}$  using the same basis

$$H_{SU(4)} = T_0 h_0 + T_8 h_8 + T_{15} h_{15} \equiv \frac{1}{2} \begin{pmatrix} h_x & 0 & 0 & 0 \\ 0 & h_x & 0 & 0 \\ 0 & 0 & \sqrt{2}h_s & 0 \\ 0 & 0 & 0 & \sqrt{2}h_c \end{pmatrix}. \quad (19)$$

Finally, the tree-level SU(4) mesonic potential in new basis reads as

$$U(\sigma_x, \sigma_y, \sigma_c) = \frac{1}{2}m^2(\sigma_x^2 + \sigma_y^2 + \sigma_c^2) - \frac{c}{4}\sigma_x^2\sigma_y\sigma_c + \frac{\lambda_1}{2}(\sigma_x^2\sigma_y^2 + \sigma_x^2\sigma_c^2 + \sigma_y^2\sigma_c^2) + \frac{1}{8}(2\lambda_1 + \lambda_2)\sigma_x^4 + \frac{1}{4}(\lambda_1 + \lambda_2)\sigma_y^4 + \frac{1}{4}(\lambda_1 + \lambda_2)\sigma_c^4 - h_x\sigma_x - h_y\sigma_y - h_c\sigma_c + \epsilon_c\sigma_c^2. \quad (20)$$

The global minima, defined by the absence of partial derivatives related to  $\sigma_x$ ,  $\sigma_y$ , and  $\sigma_c$ , define the values of  $h_x$ ,  $h_y$ ,  $h_c$ ,

$$h_x = m^2\sigma_x - \frac{c}{2}\sigma_x\sigma_y\sigma_c + \lambda_1\sigma_x(\sigma_y^2 + \sigma_c^2) + \frac{1}{2}(2\lambda_1 + \lambda_2)\sigma_x^3, \quad (21)$$

$$h_y = m^2\sigma_y - \frac{c}{4}\sigma_x^2\sigma_c + \lambda_1\sigma_y(\sigma_x^2 + \sigma_c^2) + (\lambda_1 + \lambda_2)\sigma_y^3, \quad (22)$$

$$h_c = m^2\sigma_c + 2\epsilon_c\sigma_c - \frac{c}{4}\sigma_x^2\sigma_y + \lambda_1\sigma_c(\sigma_x^2 + \sigma_y^2) + (\lambda_1 + \lambda_2)\sigma_c^3. \quad (23)$$

The tree-level masses of mesons, defined from the quadratic terms of the Lagrangian are presented in detail in Appendix B. As previously stated, the derivation for the masses of the charmed mesonic

states requires to take into account the mass term  $-2\text{Tr}[\epsilon\Phi^\dagger\Phi]$  [41], where

$$\epsilon = \begin{pmatrix} 0 & 0 & 0 & 0 \\ 0 & 0 & 0 & 0 \\ 0 & 0 & 0 & 0 \\ 0 & 0 & 0 & \epsilon_c \end{pmatrix}, \quad (24)$$

with  $\epsilon_c = m_c^2$  and  $m_c$  is the mass of the charm quark. This term provides an additional contribution specifically to the masses of charmed mesons.

The formalism for the temperature dependence shall be elaborated in the following section. The derivation of analytical formulas for meson masses, with a focus on their behaviour at limited temperatures, will be presented.

### C. Finite Temperature Formalism

To investigate how various in-medium modifications behave, we utilize the well-established Polyakov loop extension of the LSM. In this regard, we apply the chiral Lagrangian together with the Polyakov-loop potential, formulated as  $\mathcal{L} = \mathcal{L}_{\text{chiral}} - \mathcal{U}(\phi, \phi^*, T)$ . The grand potential can be derived then in the mean field approximation [51]. Given the assumption of thermal equilibrium, the grand partition function is expressed via a path integral that includes the quark, antiquark, and meson fields

$$\mathcal{Z} = \text{Tr} \exp[-\hat{\mathcal{H}}/T] = \int \prod_a \mathcal{D}\sigma_a \mathcal{D}\pi_a \int \mathcal{D}q \mathcal{D}\bar{q} \exp \left[ \int_x \mathcal{L} \right], \quad (25)$$

where  $t$  is the time at which the system with volume  $V$  evolves and  $\int_x \equiv i \int_0^{1/T} dt \int_V d^3x$ . The partition function can be derived using the mean field approximation [52–54]. In this context, the meson fields are substituted with their expectation values, specifically  $\bar{\sigma}_a$ , within the action [55, 56]. Employing standard techniques [56], the integration over the fermionic contributions can be performed. This leads to the derivation of the effective potential for the mesons

$$\Omega(T) = \frac{-T \ln \mathcal{Z}}{V} = U(\bar{\sigma}) + \mathcal{U}(\phi, \phi^*, T) + \Omega_{\bar{q}q}, \quad (26)$$

where the fields  $\phi$  or  $\phi^*$  are a complex matrix of dimensions  $N_f \times N_f$ . This effective potential has three terms which can be elaborated as follows.

- The first term is the purely mesonic potential presented in previous sections that describes the mass spectra in vacuum.

- The second term is the Poyakov loop potential, which in this study is used in classic logarithmic form [25]. Additional information on the other potentials  $\mathcal{U}(\phi, \phi^*, T)$  can be found in Refs. [51, 57, 58].
- The third term is the mean-field quark-antiquark potential which gives an in-medium modification on masses

$$\Omega_{\bar{q}q} = -2\nu_c T \sum_f \int \frac{dp}{(2\pi)^3} E_f - 2\nu_c T \sum_f \int \frac{dp}{(2\pi)^3} (\ln g_f^+ + \ln g_f^-), \quad (27)$$

where  $\nu_c = 2N_c$  and  $f$  run all flavours,  $E_f = (p^2 + m_f^2)^{1/2}$  is the flavor dependent single particle energy of quark with mass  $m_f$  and

$$g_f^+ = 1 + 3(\phi + \phi^* e^{-E_f^+/T}) e^{-E_f^+/T} + e^{-3E_f^+/T}, \quad (28)$$

$$g_f^- = 1 + 3(\phi^* + \phi e^{-E_f^-/T}) e^{-E_f^-/T} + e^{-3E_f^-/T}. \quad (29)$$

The quark and antiquark dispersion relations are  $E_f^\pm(T, \mu_f) = E_f \mp \mu_f$ , respectively. The quark masses are defined by values of the  $\sigma$ -fields:

$$m_x = \frac{g}{2}\sigma_x, \quad m_s = \frac{g}{\sqrt{2}}\sigma_y, \quad m_c = \frac{g}{\sqrt{2}}\sigma_c.$$

The masses of the various states can be determined from the second derivative of the grand potential with respect to the corresponding fields, evaluated at the potential minimum [24, 25, 32]. In the present work, these minima are defined by vanishing expectation values for all scalar, pseudoscalar, vector, and axial-vector fields [52]

$$(m_i^2)_{ab} = \left. \frac{\partial^2 \Omega}{\partial \varphi_{i,a} \partial \varphi_{i,b}} \right|_{\min}, \quad (30)$$

where  $\varphi_{i,a}$  and  $\varphi_{i,b}$  are the corresponding mass fields of the  $i$ -th hadron state. Assuming that the contribution of the quark-antiquark potential to the Lagrangian vanishes in the vacuum, the mass matrix in hot and dense matter should be extended by the additional term [52]

$$(m_i^2)_{ab} = \left. \frac{\partial^2 U(\bar{\sigma})(T, \mu)}{\partial \varphi_{i,a} \partial \varphi_{i,b}} \right|_{\min} + \left. \frac{\partial^2 \Omega_{q\bar{q}}(T, \mu)}{\partial \varphi_{i,a} \partial \varphi_{i,b}} \right|_{\min}, \quad (31)$$

where  $i$  stands for (pseudo)scalar and (axial)vector mesons and  $a$  and  $b$  are integers ranging from 0 to  $(N_f^2 - 1)$ . The first term in Eq. (31) is related to the vacuum, where the meson masses are developed from the sigma fields. The second term gives the in-medium modification on the masses of various meson states

$$\begin{aligned} \frac{\partial^2 \Omega_{q\bar{q}}(T, \mu)}{\partial \varphi_{i,a} \partial \varphi_{i,b}} = & \nu_c \sum_f \int_0^\infty \frac{dp}{(2\pi)^3} \frac{1}{2E_f} \left[ (n_f^+ + n_f^-) \left( m_{f,ab}^2 - \frac{m_{f,a}^2 m_{f,b}^2}{2E_f^2} \right) \right. \\ & \left. + (b_f^+ + b_f^-) \left( \frac{m_{f,a}^2 m_{f,b}^2}{2E_f T} \right) \right], \end{aligned} \quad (32)$$

The expression Eq. (32) contains some notations for the quark mass first derivative with respect to the meson fields  $m_{f,a}^2 \equiv \partial m_f^2 / \partial \varphi_{i,a}$  and the second derivative of the quark mass with respect to meson fields  $m_{f,ab}^2 \equiv \partial m_f^2 / \partial \varphi_{i,a} \partial \varphi_{i,b}$ . The values of these derivatives for SU(3) configuration can be found, for example, in Refs. [52, 59] and for SU(4) case are presented in Appendix C, Tab. A4. The notations  $n_f^\pm$  and  $b_f^\pm$  have the following definitions [24, 25, 32]

$$n_f^+ = \frac{\phi e^{-E_f^+/T} + 2\phi^* e^{-2E_f^+/T} + e^{-3E_f^+/T}}{1 + 3(\phi + \phi^* e^{-E_f^+/T}) e^{-E_f^+/T} + e^{-3E_f^+/T}}, \quad (33)$$

$$n_f^- = \frac{\phi^* e^{-E_f^-/T} + 2\phi e^{-2E_f^-/T} + e^{-3E_f^-/T}}{1 + 3(\phi^* + \phi e^{-E_f^-/T}) e^{-E_f^-/T} + e^{-3E_f^-/T}}. \quad (34)$$

The normalization factors for quarks and antiquarks are  $b_f^\pm = 3(n_f^\pm)^2 - c_f^\pm$  where [24, 25, 32]

$$c_f^+ = \frac{\phi e^{-E_f^+/T} + 4\phi^* e^{-2E_f^+/T} + 3e^{-3E_f^+/T}}{1 + 3(\phi + \phi^* e^{-E_f^+/T}) e^{-E_f^+/T} + e^{-3E_f^+/T}}, \quad (35)$$

$$c_f^- = \frac{\phi^* e^{-E_f^-/T} + 4\phi e^{-2E_f^-/T} + 3e^{-3E_f^-/T}}{1 + 3(\phi^* + \phi e^{-E_f^-/T}) e^{-E_f^-/T} + e^{-3E_f^-/T}}. \quad (36)$$

The numerical results are introduced in the following section. The procedure for parameter fitting shall be introduced.

### III. Results

The Lagrangian of eLSM, given in Eqs. (1-5), contains a large number of parameters:

$$m_0^2, m_1^2, c, \delta_x, \delta_y, \delta_c, g_1, g_2, g_3, g_4, g_5, g_6, h_x, h_y, h_c, h_1, h_2, h_3, \lambda_1, \lambda_2.$$

In this study, the coupling of the glueball to other mesons is neglected. Furthermore, the parameters  $g_2, g_3, g_4, g_5$  and  $g_6$  in Eq. (3) are not discussed in this work and therefore are not considered in the fit. Fitting these parameters requires fixing some meson masses and decay constants. The remaining masses and decay constants are then obtained from the fit itself.

The condensate values in vacuum are computed from the meson decay constants using the partially conserved axial-vector current relation (PCAC) [47]

$$f_a = d_{aab} \bar{\sigma}_b, \quad (37)$$

with summation over  $b$  and  $d_{abc}$  is the standard symmetric structure constants of SU( $N$ ). The  $\sigma_x$  and  $\sigma_y$  are defined by the pion and kaon decay constants. The value of  $\sigma_c$  can be expressed

in terms of the D-meson decay constant or, alternatively,  $\eta_c$  meson decay constant as  $f_{\eta_c} = 2\sigma_c$  [32, 60, 61]

$$f_\pi = \frac{\sigma_x}{Z_\pi}, \quad f_K = \frac{\sqrt{2}\sigma_y + \sigma_x}{2Z_K}, \quad f_D = \frac{\sqrt{2}\sigma_c + \sigma_x}{2Z_D}.$$

As justified in Appendix B, the factors  $Z_i$  are included in the expressions above. Table I presents the experimental data used in the fit alongside the corresponding best-fit results. We conclude that the estimation grounded in SU(4) eLSM is more consistent with experimental values than that grounded in SU(3) eLSM. This finding draws a key conclusion that an increase in quark degrees of freedom enhances the simulation accuracy of meson masses.

Observable	Experiment (MeV)	SU(3) Fit (MeV)	SU(4) Fit (MeV)
$f_\pi$	$92.2 \pm 4.6$	95.02	92.0
$f_K$	$110.4 \pm 5.5$	106.9	109.1
$f_D$	$203 \pm 5.5$	-	225.0
$m_\pi$	$137.3 \pm 6.9$	139.85	140.79
$m_K$	$495.6 \pm 24.8$	420.49	490.3
$m_\eta$	$547.9 \pm 27.4$	140.0 (531.9.0)	140.79(531.13)
$m'_\eta$	$957.8 \pm 47.9$	644.93 (965.44)	640.75(965.56)
$m_\phi$	$1019.5 \pm 51$	1019.19	1014.9
$m_\rho$	$775.5 \pm 38.8$	770.11	749.62
$m_{f_1}$	$1426.4 \pm 71.3$	1424.77	1460.39
$m_{a_1}$	$1230 \pm 62$	1069.76	1078.68
$m_{k_1}$	$1253 \pm 7$	1253.46	1276.45
$m_\sigma$	500-1200	600 (700)	745(700)
$m_{D_1}$	$2420 \pm 9$	-	2615.77

**Tab. I.** The data used for parameters fitting. In brackets are shown results for fit with  $c \neq 0$  (if differ).

The rest of the parameters are defined as follows:

- $\delta_x, \delta_y, \delta_c$  define explicit symmetry breaking in the vector and axial-vector channels, which

arises from non-vanishing quark masses. In this regard, we find the following

$$\Delta_{SU(3)} = T_0\delta_0 + T_8\delta_8 \equiv \frac{1}{2} \begin{pmatrix} \delta_x & 0 & 0 \\ 0 & \delta_x & 0 \\ 0 & 0 & \sqrt{2}\delta_s \end{pmatrix}, \quad (38)$$

$$\Delta_{SU(4)} = T_0\delta_0 + T_8\delta_8 + T_{15}\delta_{15} \equiv \frac{1}{2} \begin{pmatrix} \delta_x & 0 & 0 & 0 \\ 0 & \delta_x & 0 & 0 \\ 0 & 0 & \sqrt{2}\delta_s & 0 \\ 0 & 0 & 0 & \sqrt{2}\delta_c \end{pmatrix}. \quad (39)$$

The transition from the original octet-singlet basis to the non-strange, strange, and charm quark flavor basis is performed using the transformation matrices in Eqs. (12) and (18). These symmetry-breaking parameters are proportional to the squares of the corresponding quark masses:  $\delta_x \propto m_x^2$ ,  $\delta_y \propto m_y^2$ , and  $\delta_c \propto m_c^2$ . In the isospin-symmetric limit, we set  $\delta_x = 0$  and determine the remaining parameters  $\delta_y$  and  $\delta_c$  from the fit. The quark masses are defined by the Yukawa coupling  $g$  and the corresponding condensates. The Yukawa coupling  $g$  is fixed from the non-strange constituent quark mass as  $g = 2m_q/\sigma_x$  where  $m_q = 0.3$  GeV (see Table II).

- The parameters  $h_x$ ,  $h_y$ ,  $h_c$  define the Explicit Chiral Symmetry Breaking (ESB) in the (pseudo)scalar sector via the term  $\text{Tr}[H(\Phi + \Phi^\dagger)]$  and they are defined by the global minimum of the mesonic potential of the model (see Section II).
- The parameters  $m_1^2, g_1, h_1, h_2, h_3$  define the vector and axial-vector sectors. As can be seen from the mass expressions in Tabs. A1 and A2, the meson masses depend more significantly on the value of  $c_1$ , which can be written as

$$c_1 = m_1^2 + \frac{h_1}{2}(\sigma_x^2 + \sigma_y^2) \quad SU(3), \quad (40)$$

$$c_1 = m_1^2 + \frac{h_1}{2}(\sigma_x^2 + \sigma_y^2 + \sigma_c^2) \quad SU(4), \quad (41)$$

so that we can reduce the fit to  $g_1, h_2, h_3, c_1$ . The parameters obtained from the best fit are listed in Tab. II.

- The parameters  $m_0^2, c = 0, \lambda_1, \lambda_2$  define the scalar-pseudoscalar sector. The parameter  $c$  define the presence of the  $U(1)_A$  anomaly. For the case when  $U(1)_A$  anomaly is absent at  $c = 0$ . Accordingly, the mass of  $\eta'$  meson is identical to the pion mass. The parameter  $\lambda_2$  is

given by the kaon and pion masses. The well-known classical relation for  $\lambda_2$  reads

$$\lambda_2 = \frac{M_K^2 - M_\pi^2}{(2f_K - f_\pi)(f_K - f_\pi)}. \quad (42)$$

It is identical for both the SU(3) and SU(4) configurations. The parameters  $\lambda_1$  and  $m_0$  then can be obtained using equations for masses of the scalar sigma-meson  $m_\sigma$  and the pion mass  $m_\pi$ .

- In the presence of  $U(1)_A$  anomaly, i.e.,  $c \neq 0$ , determining the model parameters requires a system of equations constrained by the following experimental inputs:
  - the pion and kaon masses,
  - the averaged squared mass of  $\eta$  and  $\eta'$  mesons ( $m_\eta^2 + m_{\eta'}^2 = m_{\eta_N}^2 + m_{\eta_S}^2$ ), and
  - the mass of the scalar sigma-meson.

Using this solution, we can then predict the parameters, the masses of the scalar mesons  $m_{a_0}$ ,  $m_{f_0}$ , as well as the scalar and pseudoscalar mixing angles  $\theta_S$ ,  $\theta_P$ .

The parameters  $g_1$ ,  $c_1$ ,  $h_2$ ,  $h_3$ ,  $c$ ,  $m_0^2$ ,  $\lambda_1$ ,  $\lambda_2$  and  $g$  for both SU(3) and SU(4) configurations are specified in Tab. II. It is important to point out that the vacuum masses for the other mesons, which aren't included in the fit, can be found in Table IV in Appendix B.

	$g_1$	$c_1$ (GeV $^2$ )	$h_2$	$h_3$	$c$	$m_0^2$ (GeV $^2$ )	$\lambda_1$	$\lambda_2$	$g$
SU(3)	5.58	0.44	40.975	-15.216	0	$-(0.282)^2$	-10.515	55.576	5.5
					2.828	$-(0.258)^2$	3.15	36.253	
SU(4)	5.632	0.395	39.215	-13.907	0	$-(0.135)^2$	-2.115	45.54	5.217
					11.24	$-(0.707)^2$	4.055	29.19	

**Tab. II.** The best fit of the parameters  $g_1$ ,  $c_1$ ,  $h_2$ ,  $h_3$ ,  $c$ ,  $m_0^2$ ,  $\lambda_1$ ,  $\lambda_2$  and  $g$ .

Including the Polyakov potential, as introduced in II C, results in the introduction of another parameter  $T_0$ , associated with the potential. We assume  $T_0 = 0.27$  GeV, which represents the deconfinement critical temperature in the pure gauge sector. Following our previous research [32], we incorporate an additional temperature dependence for the parameter  $m_0^2$ , namely

$$m_0^2 = m_0^2 \left( 1 - \frac{T^2}{T_0^2} \right), \quad (43)$$

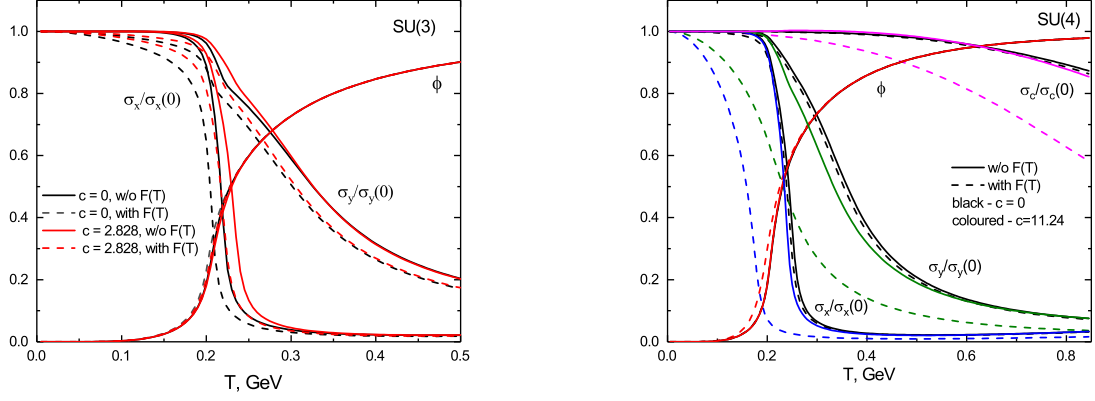


**Fig. 1.** The quark condensates for SU(3) (left panel) and SU(4) (right panel) for  $c = 0$ ,  $c \neq 0$  with (dashed lines) and without factor  $F(T) = (1 - T^2/T_0^2)$  (solid lines).

	$c = 0$	$c = 0$ with $F(T)$	$c \neq 0$	$c \neq 0$ , with $F(T)$
SU(3)	0.2175	2.075	0.2325	0.2175
SU(4)	0.2475	2.425	0.2375	0.1725

**Tab. III.** The pseudo-critical temperature of the chiral phase transition ( $T_\chi$ ) for SU(3) and SU(4) configurations with and without the factor  $F(T) = (1 - T^2/T_0^2)$ .

where  $T_0$  is proportional to the fundamental quantities of QCD, the scale for the hadron-quark confinement, i.e.,  $\Lambda_{\text{QCD}}$ , we keep  $T_0$  here also 0.27 GeV. Figure 1 shows the temperature dependence of quark condensates in the eLSM configuration with and without the factor  $F(T)$ , Eq. (43). Temperature appears to have a greater impact on light quark condensates ( $\sigma_x$ ) than strange ( $\sigma_y$ ) and charm quark condensates ( $\sigma_c$ ). The latter stays modestly temperature dependent over a large temperature range.

For the estimation of the pseudo-critical temperature of the chiral phase transition ( $T_\chi$ ), the location of the inflection point can be utilized

$$T_\chi = \left| \frac{\partial \sigma_f}{\partial T} \right|_{\max}. \quad (44)$$

Table III presents the obtained  $T_\chi$  values for all considered modifications of the model. The factor  $m_0^2$ , Eq. (43), leads to reduced  $T_\chi$  for both SU(3) and SU(4) configurations.

The figures seem to illustrate the thermal evolution of the meson mass spectrum for the pseudoscalar mesons (Fig. 3), scalar mesons (Fig. 2), vector and axial-vector mesons (Fig. 4) and open/hidden charmed mesons (Fig. 5). All are given at vanishing chemical potential  $\mu_f$ . For the pseudoscalar and scalar charmed mesons we presented only  $D$ ,  $D_s$ ,  $D_s^*$ ,  $D_{s0}^*$ , states, because masses

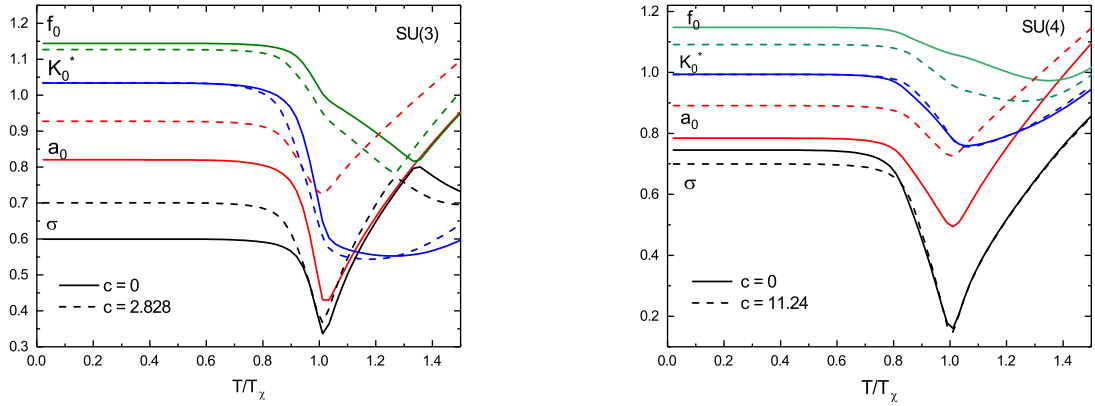


**Fig. 2.** Scalar mesons for SU(3) (left panel) and SU(4) (right panel). Meson masses are plotted both for  $c = 0$  (solid lines),  $c \neq 0$  (dashed lines) cases without involving the factor  $F(T) = (1 - T^2/T_0^2)$ .

of  $\eta_c$  meson  $m_{\eta_c} = 4.844$  GeV and  $\chi_{c0}$   $m_{\chi_{c0}} = 3.551$  GeV behave as a constant as functions of temperature in the considered temperature range. These figures allow us to conclude that while various mesonic states display specific patterns in their mass evolution with temperature, their dissociation tends to happen within a similar temperature range close to the critical temperature, with minor variations depending on the type of meson. On the other hand, the quarkonium states seem to be largely unaffected by temperature changes.

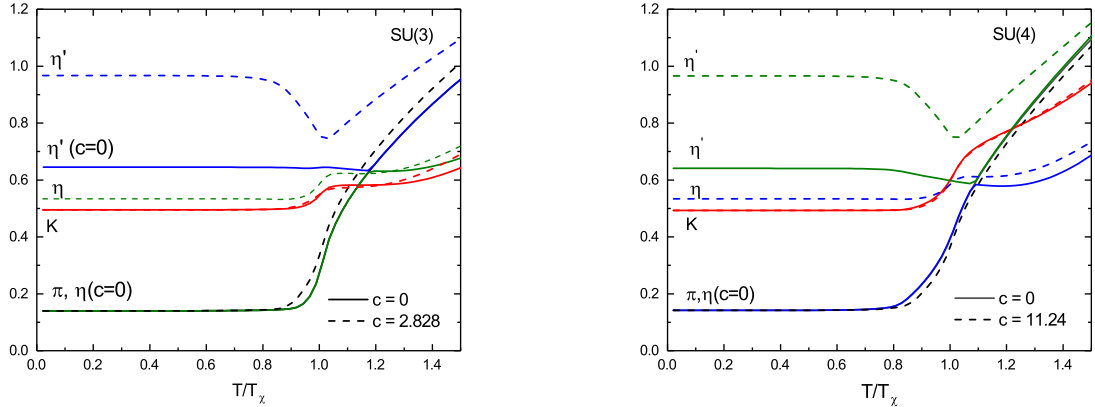


**Fig. 3.** Masses of pseudo-scalar mesons for SU(3) (left panel) and SU(4) (right panel) cases. Meson masses are plotted for  $c = 0$  (solid lines) and  $c \neq 0$  (dashed line). Meson masses presented for the case without the factor  $F(T) = (1 - T^2/T_0^2)$ .

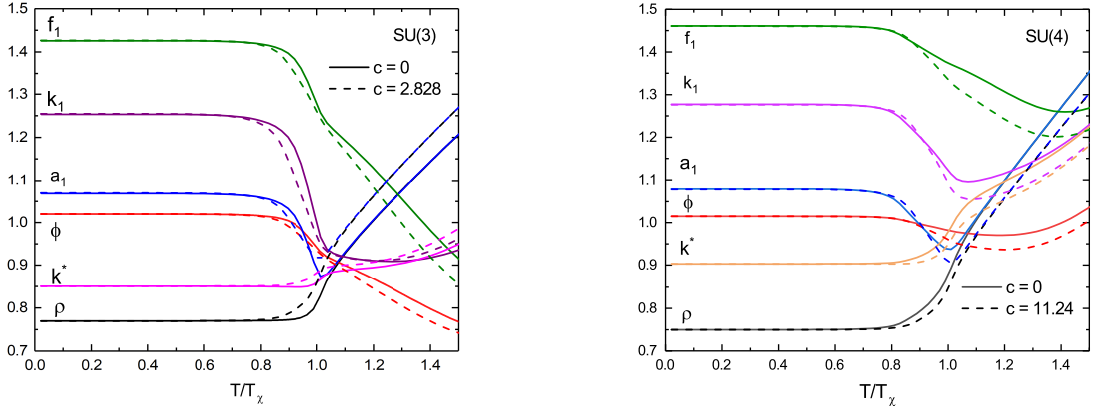


**Fig. 4.** Vector and axial-vector mesons for  $SU(3)$  (left panel) and  $SU(4)$  (right panel). Meson masses are plotted both for  $c = 0$  (solid lines),  $c \neq 0$  (dashed lines) cases without involving the factor  $F(T) = (1 - T^2/T_0^2)$ .

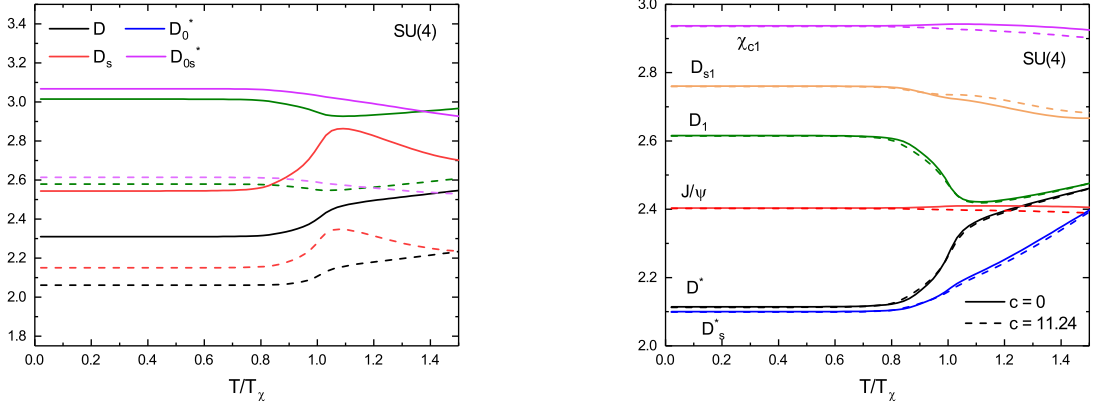


**Fig. 5.** Left panel: scalar and pseudo-scalar mesons with open charm and quarkonia. Right panel: vector and axial-vector mesons with open charm and quarkonia. Meson masses are plotted both for  $c = 0$  (solid lines),  $c \neq 0$  (dashed lines) cases without involving the factor  $F(T) = (1 - T^2/T_0^2)$ .

#### IV. Conclusion

In the extended Linear-Sigma Model, we evaluate the temperature dependence of different quark condensates, considering both the presence and absence of the factor  $F(T) = (1 - T^2/T_0^2)$ . Our results indicate that temperature significantly influences light quark condensates,  $\sigma_x$ , more than it does strange quarks,  $\sigma_y$ , and even more so than charm quark condensates,  $\sigma_c$ . This leads us to conclude that the critical temperature increases as we move from light to strange to charm quark

degrees of freedom. We also find that the effect of the  $U(1)_A$  anomaly is not the same for the  $SU(3)$  and  $SU(4)$  configurations. Given the specified parameters, the anomaly seems to increase the chiral transition temperature,  $T_\chi$ , in the  $SU(3)$  configuration, whereas it reduces it in the  $SU(4)$  configuration. Additionally, the impact of the factor  $F(T)$  is more substantial in the  $SU(4)$  configuration.

Pseudoscalar sector ( $J^P = 0^-$ )			Scalar sector ( $J^P = 0^+$ )		
Exp., GeV	$SU(3)$ , GeV	$SU(4)$ , GeV	Exp., GeV	$SU(3)$ , GeV	$SU(4)$ , GeV
$\pi$ (0.139)	0.139	0.142	$a_0$ (0.98)	0.926	0.89
$K$ (0.497)	0.42	0.493	$k$ (0.63-1.425)	1.032	0.993
$\eta$ (0.547)	0.531	0.533	$\sigma$ (0.5-1.2)	0.7	0.7
$\eta'$ (0.958)	0.965	0.966	$f_0$ (0.98-1.5)	1.124	1.091
Vector mesons ( $J^P = 1^-$ )			Axial-vector mesons ( $J^P = 1^+$ )		
$\rho$ (0.761)	0.77	0.749	$a_1$ (1.26)	1.067	1.015
$K^*$ (0.89)	0.851	0.903	$K_1$ (1.27)	1.253	1.276
$\phi$ (1.02)	1.019	1.015	$f_1$ (1.428)	1.425	1.46
Charmed mesons					
Scalar-pseudoscalar sector			Vector,axial-vector sector		
Exp., GeV	$J^P$	$SU(4)$ , GeV	Exp., GeV	$J^P$	$SU(4)$ , GeV
$\eta_c$ (2S) (3.637)	$0^-$	4.844	$J/\psi$ (3.096)	$1^-$	2.403
$D$ (1.864)	$0^-$	2.03	$D^*$ (2.007)	$1^-$	2.114
$D_s$ (1.968)	$0^-$	2.116	$D_s^*$ (2.112)	$1^-$	2.1
$\chi_{c0}$ (3.86)	$0^+$	3.551	$\chi_{c1}$ (3.414)	$1^+$	2.937
$D_0^*$ (2.343)	$0^+$	2.578	$D_1$ (2.422)	$1^+$	2.615
$D_{s0}^*$ (2.317)	$0^+$	2.293	$D_{s1}$ (2.45)	$1^+$	2.760

**Tab. IV.** A comparison between meson masses within  $SU(3)$  and  $SU(4)$  eLSM.

The various meson states including pseudoscalars ( $J^{pc} = 0^{-+}$ ), scalars ( $J^{pc} = 0^{++}$ ), vectors ( $J^{pc} = 1^{--}$ ), and axial-vectors ( $J^{pc} = 1^{++}$ ) are investigated in  $SU(3)$  and  $SU(4)$  eLSM both in vacuum and finite temperatures. The vacuum masses of the mesons are listed in Tab. IV for both configurations and compared with experimental values [62]. It is obvious that the masses involving open charm in the scalar and pseudoscalar sectors agree better with experimental values than those in the vector sector. However, the model parameters obtained here do not allow for equally good agreement for quarkonium states.

The examination of the chiral phase-structure properties for all of these mesonic states allows one to determine the in-medium modifications of hadronic matter as well as the critical tempera-

ture at which each mesonic state splits into its free quarks. This facilitates a comparison between the masses of strange and charm mesons relative to the masses of lighter mesons. The comparative analyses in SU(3) and SU(4) eLSM helps in determining the influences that brought about additional degrees of freedom and thereby the accurate estimation of the various meson states.

We conclude that the inclusion of large quark degrees of freedom, SU(4), markedly improves the precision of meson mass simulations compared to the lower quark degrees of freedom, SU(3). After establishing all fitting parameters, the temperature dependence of meson masses appears to show a striking change at the critical temperature. This investigation suggests that different mesonic states generally possess a unified range of dissolution temperatures, indicating that the critical temperature seems to vary with the meson states. We also find that the quarkonium states, which are composed of a quark and its antiquark, seem to be influenced by temperature variations.

---

[1] A. Tawfik, N. Magdy, and A. Diab. Polyakov linear SU(3)  $\sigma$  model: Features of higher-order moments in a dense and thermal hadronic medium. *Phys. Rev. C*, 89(5):055210, 2014. doi: 10.1103/PhysRevC.89.055210.

[2] Abdel Nasser Tawfik, Abdel Magied Diab, Nada Ezzelarab, and Asmaa G. Shalaby. QCD thermodynamics and magnetization in nonzero magnetic field. *Adv. High Energy Phys.*, 2016:1381479, 2016. doi:10.1155/2016/1381479.

[3] Abdel Nasser Tawfik, Abdel Magied Diab, and M. T. Hussein. Quark–hadron phase structure, thermodynamics, and magnetization of QCD matter. *J. Phys. G*, 45(5):055008, 2018. doi:10.1088/1361-6471/aaba9e.

[4] Abdel Nasser Tawfik, Abdel Magied Diab, and M. T. Hussein. SU(3) Polyakov linear-sigma model: Conductivity and viscous properties of QCD matter in thermal medium. *Int. J. Mod. Phys. A*, 31(34): 1650175, 2016. doi:10.1142/S0217751X1650175X.

[5] Heinz Pagels. Dynamical Chiral Symmetry Breaking in Quantum Chromodynamics. *Phys. Rev. D*, 19: 3080, 1979. doi:10.1103/PhysRevD.19.3080.

[6] S. GASIOROWICZ and D. A. GEFFEN. Effective lagrangians and field algebras with chiral symmetry. *Rev. Mod. Phys.*, 41:531–573, Jul 1969. doi:10.1103/RevModPhys.41.531. URL <https://link.aps.org/doi/10.1103/RevModPhys.41.531>.

[7] C. Becchi, Stephan Narison, E. de Rafael, and F. J. Yndurain. Light Quark Masses in Quantum Chromodynamics and Chiral Symmetry Breaking. *Z. Phys. C*, 8:335, 1981. doi:10.1007/BF01546328.

[8] T. L. Trueman. Chiral Symmetry in Perturbative QCD. *Phys. Lett. B*, 88:331–334, 1979. doi: 10.1016/0370-2693(79)90480-5.

[9] A. A. Osipov, B. Hiller, and A. H. Blin. Effective multiquark interactions with explicit breaking of

chiral symmetry. *Phys. Rev. D*, 88:054032, 2013. doi:10.1103/PhysRevD.88.054032.

[10] Katherine Freese, Joshua A. Frieman, and Angela V. Olinto. Natural inflation with pseudo - Nambu-Goldstone bosons. *Phys. Rev. Lett.*, 65:3233–3236, 1990. doi:10.1103/PhysRevLett.65.3233.

[11] Robert Foot, Archil Kobakhidze, and Raymond R. Volkas. Electroweak Higgs as a pseudo-Goldstone boson of broken scale invariance. *Phys. Lett. B*, 655:156–161, 2007. doi:10.1016/j.physletb.2007.06.084.

[12] Kenji Yamada, Muneyuki Ishida, Shin Ishida, Daiki Ito, Toshihiko Komada, and Hiroshi Tonooka. Possible evidence for a chiral axial vector state in the D meson system. *AIP Conf. Proc.*, 619(1):657–660, 2002. doi:10.1063/1.1482512.

[13] David J. Wilson, Christopher E. Thomas, Jozef J. Dudek, and Robert G. Edwards. Charmonium  $\chi c0$  and  $\chi c2$  resonances in coupled-channel scattering from lattice QCD. *Phys. Rev. D*, 109(11):114503, 2024. doi:10.1103/PhysRevD.109.114503.

[14] R. G. Jafarov and V. E. Rochev. Mean field expansion and meson effects in chiral condensate of analytically regularized Nambu-Jona-Lasinio model. *Central Eur. J. Phys.*, 2:367–381, 2004. doi:10.2478/BF02475637.

[15] M. Matsuo and T. Matsui. Quantized meson fields in and out of equilibrium. II: Chiral condensate and collective meson excitations. 12 2008.

[16] Zheng Zhang, Chao Shi, and Hong-Shi Zong. Nambu-jona-lasinio model in a sphere. *Phys. Rev. D*, 101:043006, Feb 2020. doi:10.1103/PhysRevD.101.043006.

[17] Christian S. Fischer. Qcd at finite temperature and chemical potential from dyson-schwinger equations. *Progress in Particle and Nuclear Physics*, 105:1–60, 2019. doi: <https://doi.org/10.1016/j.ppnp.2019.01.002>.

[18] Alejandro Ayala, Adnan Bashir, C. A. Dominguez, Enif Gutiérrez, M. Loewe, and Alfredo Raya. Qcd phase diagram from finite energy sum rules. *Phys. Rev. D*, 84:056004, 2011. doi:10.1103/PhysRevD.84.056004.

[19] D. Espriu, A.G. Nicola, and Vioque-Rodríguez. A. chiral perturbation theory for nonzero chiral imbalance. *J. High Energ. Phys.*, 2020:62, 2020. doi:[https://doi.org/10.1007/JHEP06\(2020\)062](https://doi.org/10.1007/JHEP06(2020)062).

[20] F. Karsch, K. Redlich, and A. Tawfik. Hadron resonance mass spectrum and lattice QCD thermodynamics. *Eur. Phys. J. C*, 29:549–556, 2003. doi:10.1140/epjc/s2003-01228-y.

[21] F. Karsch, K. Redlich, and A. Tawfik. Thermodynamics at nonzero baryon number density: A Comparison of lattice and hadron resonance gas model calculations. *Phys. Lett. B*, 571:67–74, 2003. doi:10.1016/j.physletb.2003.08.001.

[22] Ya-Peng Zhao. Thermodynamic properties and transport coefficients of qcd matter within the nonextensive polyakov–nambu–jona–lasinio model. *Phys. Rev. D*, 101:096006, 2020. doi:10.1103/PhysRevD.101.096006.

[23] Michael Buballa. Njl-model analysis of dense quark matter. *Physics Reports*, 407(4):205–376, 2005. doi:<https://doi.org/10.1016/j.physrep.2004.11.004>.

[24] Abdel Nasser Tawfik and Abdel Magied Diab. Polyakov SU(3) extended linear-  $\sigma$  model:

Sixteen mesonic states in chiral phase structure. *Phys. Rev. C*, 91(1):015204, 2015. doi:10.1103/PhysRevC.91.015204.

[25] Abdel Nasser Tawfik, Abdel Magied Diab, and M. T. Hussein. Chiral phase structure of the sixteen meson states in the SU(3) Polyakov linear-sigma model for finite temperature and chemical potential in a strong magnetic field. *Chin. Phys. C*, 43(3):034103, 2019. doi:10.1088/1674-1137/43/3/034103.

[26] Susanna Gallas, Francesco Giacosa, and Dirk H. Rischke. Vacuum phenomenology of the chiral partner of the nucleon in a linear sigma model with vector mesons. *Phys. Rev. D*, 82:014004, Jul 2010. doi:10.1103/PhysRevD.82.014004.

[27] Denis Parganlija, Francesco Giacosa, and Dirk H. Rischke. Vacuum properties of mesons in a linear sigma model with vector mesons and global chiral invariance. *Phys. Rev. D*, 82:054024, Sep 2010. doi:10.1103/PhysRevD.82.054024.

[28] Stanislaus Janowski, Denis Parganlija, Francesco Giacosa, and Dirk H. Rischke. Glueball in a chiral linear sigma model with vector mesons. *Phys. Rev. D*, 84:054007, Sep 2011. doi:10.1103/PhysRevD.84.054007.

[29] Stephan Narison. Light and Heavy Quark Masses, Test of PCAC and Flavor Breakings of Condensates in QCD. *Phys. Lett. B*, 216:191–197, 1989. doi:10.1016/0370-2693(89)91393-2.

[30] G. 't Hooft. Symmetry breaking through bell-jackiw anomalies. *Phys. Rev. Lett.*, 37:8–11, Jul 1976. doi:10.1103/PhysRevLett.37.8.

[31] D. Parganlija, P. Kovács, Gy. Wolf, F. Giacosa, and D. H. Rischke. Meson vacuum phenomenology in a three-flavor linear sigma model with (axial-)vector mesons. *Phys. Rev. D*, 87:014011, Jan 2013. doi:10.1103/PhysRevD.87.014011.

[32] Abdel Nasser Tawfik, Azar I. Ahmadov, Alexandra Friesen, Yuriy Kalinovsky, Alexey Aparin, and Mahmoud Hanafy. Derivation of Meson Masses in SU(3) and SU(4) Extended Linear Sigma Model at Finite Temperature. *Particles*, 8(1):9, 2025. doi:10.3390/particles8010009.

[33] R. Vertesi, T. Csorgo, and J. Sziklai. Significant in-medium  $\eta'$  mass reduction in  $\sqrt{s_{NN}} = 200$  GeV Au+Au collisions at the BNL Relativistic Heavy Ion Collider. *Phys. Rev. C*, 83:054903, 2011. doi:10.1103/PhysRevC.83.054903.

[34] W. Cassing. Transport analysis of in-medium hadron effects in pA and AA collisions. *Eur. Phys. J. A*, 18:467, 2003. doi:10.1140/epja/i2002-10261-y.

[35] Andrea Dainese. Perspectives for the study of charm in-medium quenching at the LHC with ALICE. *Eur. Phys. J. C*, 33:495–503, 2004. doi:10.1140/epjc/s2004-01645-4.

[36] A. Tawfik. In-medium modifications of hadron properties. *Indian J. Phys.*, 85:755–766, 2011. doi:10.1007/s12648-011-0074-y.

[37] J. Friese. Studying in-medium hadron properties with HADES. *Prog. Part. Nucl. Phys.*, 42:235–245, 1999. doi:10.1016/S0146-6410(99)00079-4.

[38] L. Tolos, J. Schaffner-Bielich, and H. Stoecker. D-mesons: In-medium effects at FAIR. *Phys. Lett. B*, 635:85–92, 2006. doi:10.1016/j.physletb.2006.02.045.

[39] D. Finogeev, M. Golubeva, F. Guber, A. Ivashkin, A. Izvestnyy, N. Karpushkin, S. Morozov, and A. Reshetin. The PSD CBM Supermodule Response Study for Hadrons in Momentum Range 2 – 6 GeV/c at CERN Test Beams. *KnE Energ. Phys.*, 3:333–339, 2018. doi:10.18502/ken.v3i1.1763.

[40] Petr Parfenov, Dim Idrisov, Vinh Ba Luong, Nikolay Geraksiev, Anton Truttse, and Alexander Demanov. Anisotropic Flow Measurements of Identified Hadrons with MPD Detector at NICA. *Particles*, 4(2):146–158, 2021. doi:10.3390/particles4020014.

[41] F. Giacosa, D. Parganlija, P. Kovacs, and G. Wolf. *Eur. Phys. J. Web Conf.*, 37:08006, 2012.

[42] J. A. Mignaco and E. Remiddi. On the renormalization of the linear sigma-model. *Nuovo Cim. A*, 1:376–394, 1971. doi:10.1007/BF02723268.

[43] C. Contreras and M. Loewe. The Linear  $\sigma$  Model and Finite Temperature Effects. *Int. J. Mod. Phys. A*, 5:2297, 1990. doi:10.1142/S0217751X90001069.

[44] A. Bhattacharyya and S. Raha. Temperature dependence of hadron masses. 1: Results from an extended linear sigma model. *J. Phys. G*, 21:741–750, 1995. doi:10.1088/0954-3899/21/6/004.

[45] Heui-Seol Roh and T. Matsui. Chiral phase transition at finite temperature in the linear sigma model. *Eur. Phys. J. A*, 1:205–220, 1998. doi:10.1007/s100500050050.

[46] Robert Delbourgo and M. D. Scadron. Dynamical generation of linear sigma model SU(3) Lagrangian and meson nonet mixing. *Int. J. Mod. Phys. A*, 13:657, 1998. doi:10.1142/S0217751X98000299.

[47] Jonathan T. Lenaghan, Dirk H. Rischke, and Jurgen Schaffner-Bielich. Chiral symmetry restoration at nonzero temperature in the SU(3)(r)  $\times$  SU(3)(l) linear sigma model. *Phys. Rev. D*, 62:085008, 2000. doi:10.1103/PhysRevD.62.085008.

[48] Azar I. Ahmadov, Azza A. Alshehri, and Abdel Nasser Tawfik. Mass Spectrum of Non-Charmed and Charmed Meson States in Extended Linear-Sigma Model. *Particles*, 7:560–575, 2024. doi:10.3390/particles7030031.

[49] R.E. Mott.  $Su(4) \times su(4)$  symmetry breaking and its implications for  $su(3) \times su(3)$  breaking. *Nuclear Physics B*, 84(1):260–268, 1975. ISSN 0550-3213. doi:[https://doi.org/10.1016/0550-3213\(75\)90550-7](https://doi.org/10.1016/0550-3213(75)90550-7). URL <https://www.sciencedirect.com/science/article/pii/0550321375905507>.

[50] Joyce C. Myers and Michael C. Ogilvie. New phases of  $su(3)$  and  $su(4)$  at finite temperature. *Phys. Rev. D*, 77:125030, Jun 2008. doi:10.1103/PhysRevD.77.125030. URL <https://link.aps.org/doi/10.1103/PhysRevD.77.125030>.

[51] Abdel Nasser Tawfik, Carsten Greiner, Abdel Magied Diab, M. T. Ghoneim, and H. Anwer. Polyakov linear- $\sigma$  model in mean-field approximation and optimized perturbation theory. *Phys. Rev. C*, 101(3):035210, 2020. doi:10.1103/PhysRevC.101.035210.

[52] Bernd-Jochen Schaefer and Mathias Wagner. The Three-flavor chiral phase structure in hot and dense QCD matter. *Phys. Rev. D*, 79:014018, 2009. doi:10.1103/PhysRevD.79.014018.

[53] Bernd-Jochen Schaefer and Jochen Wambach. Susceptibilities near the QCD (tri)critical point. *Phys. Rev. D*, 75:085015, 2007. doi:10.1103/PhysRevD.75.085015.

[54] O. Scavenius, A. Mocsy, I. N. Mishustin, and D. H. Rischke. Chiral phase transition within effective

models with constituent quarks. *Phys. Rev. C*, 64:045202, 2001. doi:10.1103/PhysRevC.64.045202.

[55] M. Cheng et al. The QCD equation of state with almost physical quark masses. *Phys. Rev. D*, 77: 014511, 2008. doi:10.1103/PhysRevD.77.014511.

[56] J. I. Kapusta and Charles Gale. *Finite-temperature field theory: Principles and applications*. Cambridge Monographs on Mathematical Physics. Cambridge University Press, 2011. ISBN 978-0-521-17322-3, 978-0-521-82082-0, 978-0-511-22280-1. doi:10.1017/CBO9780511535130.

[57] Abdel Nasser Tawfik, Abdel Magied Diab, M. T. Ghoneim, and H. Anwer. SU(3) Polyakov Linear-Sigma Model With Finite Isospin Asymmetry: QCD Phase Diagram. *Int. J. Mod. Phys. A*, 34(31): 1950199, 2019. doi:10.1142/S0217751X19501999.

[58] Abdel Nasser Tawfik and Abdel Magied Diab. Chiral magnetic properties of QCD phase-diagram. *Eur. Phys. J. A*, 57(6):200, 2021. doi:10.1140/epja/s10050-021-00501-z.

[59] Uma Shankar Gupta and Vivek Kumar Tiwari. Meson Masses and Mixing Angles in 2+1 Flavor Polyakov Quark Meson Sigma Model and Symmetry Restoration Effects. *Phys. Rev. D*, 81:054019, 2010. doi:10.1103/PhysRevD.81.054019.

[60] Abdel Magied Diab. Charmed Meson Structure across Crossover from SU(4) Polyakov Quark Meson Model with Isospin Asymmetry. 5 2025. doi:10.1088/1674-1137/ae042d.

[61] Walaa I. Eshraim, Francesco Giacosa, and Dirk H. Rischke. Phenomenology of charmed mesons in the extended Linear Sigma Model. *Eur. Phys. J. A*, 51(9):112, 2015. doi:10.1140/epja/i2015-15112-2.

[62] S. Navas et al. Review of particle physics. *Phys. Rev. D*, 110(3):030001, 2024. doi:10.1103/PhysRevD.110.030001.

[63] Denis Parganlija, Peter Kovacs, Gyorgy Wolf, Francesco Giacosa, and Dirk H. Rischke. Meson vacuum phenomenology in a three-flavor linear sigma model with (axial-)vector mesons. *Phys. Rev. D*, 87(1): 014011, 2013. doi:10.1103/PhysRevD.87.014011.

[64] D. Parganlija, P. Kovács, Gy. Wolf, F. Giacosa, and D. H. Rischke. Meson vacuum phenomenology in a three-flavor linear sigma model with (axial-)vector mesons. *Physical Review D*, 87(1), January 2013. ISSN 1550-2368. doi:10.1103/physrevd.87.014011. URL <http://dx.doi.org/10.1103/PhysRevD.87.014011>.

[65] H. Navelet. THE ETA, ETA-prime, ETA(c) MIXING ANGLES AND SU(4). *Z. Phys. C*, 5:325–331, 1980. doi:10.1007/BF01557820.

[66] Yu-Jie Zhang, Xing-Gang Wu, Dan-Dan Hu, and Long Zeng.  $\eta - \eta'$  mixing and its application in the  $B+, D+, Ds+ \rightarrow \eta(\eta')\ell + \nu\ell$  decays. *Phys. Rev. D*, 112(7):076001, 2025. doi:10.1103/b51l-qdlg.

[67] T. Feldmann, P. Kroll, and B. Stech. Mixing and decay constants of pseudoscalar mesons. *Phys. Rev. D*, 58:114006, 1998. doi:10.1103/PhysRevD.58.114006.

[68] B. Bagchi, P. Bhattacharyya, S. Sen, and J. Chakrabarti. Mixing angles and decay constants of  $\eta$ ,  $\eta'$ , and  $\eta_c$ . *Phys. Rev. D*, 60:074002, Aug 1999. doi:10.1103/PhysRevD.60.074002. URL <https://link.aps.org/doi/10.1103/PhysRevD.60.074002>.

[69] Camilla Di Donato, Giulia Ricciardi, and Ikaros Bigi.  $\eta - \eta'$  Mixing - From electromagnetic

transitions to weak decays of charm and beauty hadrons. *Phys. Rev. D*, 85:013016, 2012. doi: 10.1103/PhysRevD.85.013016.

[70] Eberhard Klempt. Glueballs, hybrids, pentaquarks: Introduction to hadron spectroscopy and review of selected topics. In *18th Annual Hampton University Graduate Studies*, 4 2004.

[71] Walaa I. Eshraim, Francesco Giacosa, and Dirk H. Rischke. Phenomenology of charmed mesons in the extended linear sigma model. *Eur. Phys. J. A*, 51(9):112, 2015.

### A. Tree-Level masses

Let us now consider the scalar-pseudoscalar term of the Lagrangian equation (2) that includes the determinant term  $c[\det\Phi + \det\bar{\Phi}]$  as shown in Eq. (5) with  $c_0 = c_1 = 0$ . If we consider that  $\sigma_0$  and  $\sigma_8$  fields have nonzero vacuum expectation values ( $\bar{\sigma}_0$  and  $\bar{\sigma}_8$ ), and we adjust these fields according to their expectation values [47], then the tree-level potential of the LSM in a general structure can be expressed as

$$U(\bar{\sigma}) = \frac{m^2}{2}\bar{\sigma}_a^2 - [3\delta(N_f, 2)\mathcal{G}_{ab} + \delta(N_f, 3)\mathcal{G}_{abc}\bar{\sigma}_c]\bar{\sigma}_a\bar{\sigma}_b + \frac{1}{3}[\mathcal{F}_{abcd} + \delta(N_f, 4)\mathcal{G}_{abcd}]\bar{\sigma}_a\bar{\sigma}_b\bar{\sigma}_c\bar{\sigma}_d - h_a\bar{\sigma}_a, \quad (\text{A1})$$

where  $\mathcal{G}_{ab}$ ,  $\mathcal{G}_{abc}$ ,  $\mathcal{G}_{abcd}$ ,  $\mathcal{F}_{abcd}$ ,  $\mathcal{H}_{abcd}$  are defined in the following way

$$\mathcal{G}_{ab} = \frac{c}{6}[\delta_{a0}\delta_{b0} - \delta_{a1}\delta_{b1} - \delta_{a2}\delta_{b2} - \delta_{a3}\delta_{b3}], \quad (\text{A2})$$

$$\mathcal{G}_{abc} = \frac{c}{6}\left[d_{abc} - \frac{3}{2}(\delta_{a0}d_{0bc} + \delta_{b0}d_{a0c} + \delta_{c0}d_{ab0}) + \frac{9}{2}d_{000}\delta_{a0}\delta_{b0}\delta_{c0}\right], \quad (\text{A3})$$

$$\begin{aligned} \mathcal{G}_{abcd} = & \frac{c}{16}\left[\delta_{ab}\delta_{cd} + \delta_{ad}\delta_{bc} + \delta_{ac}\delta_{bd} - (d_{abn}d_{ncd} + d_{adn}d_{nbc} + d_{acn}d_{nbd}) + 16\delta_{a0}\delta_{b0}\delta_{c0}\delta_{d0}\right] \\ & - 4(\delta_{a0}\delta_{b0}\delta_{cd} + \delta_{a0}\delta_{c0}\delta_{bd} + \delta_{a0}\delta_{d0}\delta_{bc} + \delta_{b0}\delta_{c0}\delta_{ad} + \delta_{b0}\delta_{d0}\delta_{ac} + \delta_{c0}\delta_{d0}\delta_{ab}) \\ & + \sqrt{8}(\delta_{a0}d_{bcd} + \delta_{b0}d_{cda} + \delta_{c0}d_{dab} + \delta_{d0}d_{abc}), \end{aligned} \quad (\text{A4})$$

$$\mathcal{F}_{abcd} = \frac{\lambda_1}{4}(\delta_{ab}\delta_{cd} + \delta_{ad}\delta_{bc} + \delta_{ac}\delta_{bd}) + \frac{\lambda_2}{8}(d_{abn}d_{ncd} + d_{adn}d_{nbc} + d_{acn}d_{nbd}), \quad (\text{A5})$$

$$\mathcal{H}_{abcd} = \frac{\lambda_1}{4}\delta_{ab}\delta_{cd} + \frac{\lambda_2}{8}(d_{abn}d_{ncd} + f_{acn}f_{nbd} + f_{bcn}f_{nad}). \quad (\text{A6})$$

The standard antisymmetric and symmetric structure constants of  $SU(N)$  are represented by  $f_{abc}$  and  $d_{abc}$  respectively, where  $a, b, c = 1, \dots, N_c^2 - 1$ , with  $N_c$  being the degrees of freedom for colors.

The tree-level masses of pseudoscalars  $(m_P^2)_{ab}$  and scalars  $(m_S^2)_{ab}$  are determined from the quadratic components of the Lagrangian and, in the general  $SU(2)$ - $SU(4)$  configurations, can be expressed as

$$(m_S^2)_{ab} = m^2\delta_{ab} - 6[\delta(N_f, 2)\mathcal{G}_{ab} + \delta(N_f, 3)\mathcal{G}_{abc}\bar{\sigma}_c] + 4[\mathcal{F}_{abcd} + \delta(N_f, 4)\mathcal{G}_{abcd}]\bar{\sigma}_c\bar{\sigma}_d, \quad (\text{A7})$$

$$(m_P^2)_{ab} = m^2\delta_{ab} + 6[\delta(N_f, 2)\mathcal{G}_{ab} + \delta(N_f, 3)\mathcal{G}_{abc}\bar{\sigma}_c] + 4[\mathcal{F}_{abcd} - \delta(N_f, 4)\mathcal{G}_{abcd}]\bar{\sigma}_c\bar{\sigma}_d. \quad (\text{A8})$$

Here, the summation runs over the index  $n$  only. For the sake of simplicity, the bar notation will be omitted hereafter. Equations for vector and axial-vector mesons are defined as

$$(m_V^2)_{ab} = m_1^2 + J_{abmn}\sigma_m\sigma_n, \quad (\text{A9})$$

$$(m_A^2)_{ab} = m_1^2 + J'_{abmn}\sigma_m\sigma_n, \quad (\text{A10})$$

where  $a, b$  refer to the meson state, and the summation runs over  $m, n \in \{1, 2, \dots, (N_c^2 - 1)\}$  [63]. The coefficients  $J_{abcd}$  and  $J'_{abcd}$  are given as follows

$$\begin{aligned} J_{abcd} &= g_1^2 f_{acn} f_{bdn} + \frac{h_1}{2} \delta_{ab} \delta_{cd} + \frac{h_2}{2} d_{abn} d_{cdn} \\ &+ \frac{h_3}{2} (d_{acn} d_{bdn} + d_{adn} d_{bcn} - f_{acn} f_{bdn} - f_{adn} f_{bcn}), \end{aligned} \quad (\text{A11})$$

$$\begin{aligned} J'_{abcd} &= g_1^2 d_{acn} d_{bdn} + \frac{h_1}{2} \delta_{ab} \delta_{cd} + \frac{h_2}{2} d_{abn} d_{cdn} \\ &- \frac{h_3}{2} (d_{acn} d_{bdn} + d_{adn} d_{bcn} - f_{acn} f_{bdn} - f_{adn} f_{bcn}). \end{aligned} \quad (\text{A12})$$

Again, the sum operates solely over the index  $n$ , while  $d_{abc}$  and  $f_{abc}$  represent the symmetric and antisymmetric structure constants of  $U(N_f)$ , respectively. It should be noticed that all the resulting expressions are converted to the nonstrange-strange and the nonstrange-strange-charm basis as it was discussed in Section II A and Section II B.

Furthermore, it should be emphasized that due to the mixing between the (pseudo)scalar and (axial)vector sector through the covariant derivative, Eq. (7), the tree-level expressions of the pseudoscalars and some scalars are not mass eigenstates. It was reported that when the corresponding wave functions are renormalized to the constants  $Z_i$ , such a mixing can be resolved [64]. The factors  $Z_i$  are now emerging in mass expressions [32]

$$\begin{aligned} Z_\pi &= Z_{\eta_N} = \frac{m_{a_1}}{\sqrt{m_{a_1}^2 - g_1^2 \sigma_x^2}}, & Z_K &= \frac{2m_{K_1}}{\sqrt{4m_{K_1}^2 - g_1^2 (\sigma_x + \sqrt{2}\sigma_y)^2}}, \\ Z_{\eta_S} &= \frac{m_{f_{1S}}}{\sqrt{m_{f_{1S}}^2 - 2g_1^2 \sigma_y^2}}, & Z_{K_0^*} &= \frac{2m_{K_0^*}}{\sqrt{4m_{K_0^*}^2 - g_1^2 (\sigma_x - \sqrt{2}\sigma_y)^2}}, \\ Z_{k_s} &= \frac{2m_K}{\sqrt{4m_K^2 - g_1^2 (\sigma_x + \sqrt{2}\sigma_y)^2}}. \end{aligned}$$

And for charmed mesons, the factors  $Z_i$  read [32]

$$\begin{aligned} Z_{\eta_c} &= \frac{m_{\chi_{c1}}}{\sqrt{m_{\chi_{c1}}^2 - 2g_1^2 \sigma_c^2}}, & Z_D &= \frac{2m_{D_1}}{\sqrt{4m_{D_1}^2 - g_1^2 (\sigma_x + \sqrt{2}\sigma_c)^2}}, \\ Z_{D_s} &= \frac{\sqrt{2}m_{D_{s1}}}{\sqrt{2m_{D_{s1}}^2 - g_1^2 (\sigma_y + \sigma_c)^2}}, & Z_{D_0^*} &= \frac{2m_{D^*}}{\sqrt{4m_{D^*}^2 - g_1^2 (\sigma_x - \sqrt{2}\sigma_c)^2}}, \\ Z_{D_0^{*0}} &= \frac{2m_{D^{*0}}}{\sqrt{4m_{D^{*0}}^2 - g_1^2 (\sigma_x - \sqrt{2}\sigma_c)^2}}, & Z_{D_{s0}^*} &= \frac{\sqrt{2}m_{D_s^*}}{\sqrt{2m_{D_s^*}^2 - g_1^2 (\sigma_y - \sigma_c)^2}}. \end{aligned}$$

## B. Meson states

For the  $N_f = 3$  the identification of the physical scalar and pseudoscalar fields is given as

$$T_a \sigma_a = \frac{1}{\sqrt{2}} \begin{pmatrix} \frac{1}{\sqrt{2}}a_0^0 + \frac{1}{\sqrt{6}}\sigma_8 + \frac{1}{\sqrt{3}}\sigma_0 & a_0^+ & \kappa^+ \\ a_0^- & -\frac{1}{\sqrt{2}}a_0^0 + \frac{1}{\sqrt{3}}\sigma_0 + \frac{1}{\sqrt{6}}\sigma_8 & \kappa^0 \\ \kappa^- & \bar{\kappa}^0 & -\frac{2}{\sqrt{6}}\sigma_8 + \frac{1}{\sqrt{3}}\sigma_0 \end{pmatrix}, \quad (B1)$$

$$T_a \pi_a = \frac{1}{\sqrt{2}} \begin{pmatrix} \frac{1}{\sqrt{2}}\pi^0 + \frac{1}{\sqrt{6}}\pi_8 + \frac{1}{\sqrt{3}}\pi_0 & \pi^+ & K^+ \\ \pi^- & -\frac{1}{\sqrt{2}}\pi^0 + \frac{1}{\sqrt{6}}\pi_8 + \frac{1}{\sqrt{3}}\pi_0 & K^- \\ K^- & \bar{K}^0 & -\frac{2}{\sqrt{6}}\pi_8 + \frac{1}{\sqrt{3}}\pi_0 \end{pmatrix}. \quad (B2)$$

Here  $\pi^\pm = (\pi_1 \mp i\pi_2)/\sqrt{2}$  and  $\pi^0 = \pi_3$  are the pions,  $K^\pm = (\pi_4 \mp i\pi_5/\sqrt{2})$ ,  $K^0 = (\pi_6 - i\pi_7/\sqrt{2})$ ,  $\bar{K}^0 = (\pi_6 + i\pi_7/\sqrt{2})$  are the kaons. The  $\pi_0$  and the  $\pi_8$  are admixtures of the  $\eta$  and  $\eta'$  mesons, while  $\kappa$  can be identified as the parity partner of the kaon. The fields  $\sigma_0$  and  $\sigma_8$  correspond to admixtures of the  $\sigma$  and  $f_0$  mesons. The mixing of isoscalar states in pseudoscalar and scalar SU(3) multiplets is described in detail in Refs. [52, 64].

For  $N_f = 4$  we use the following matrices

$$T_a \sigma_a = \frac{1}{\sqrt{2}} \begin{pmatrix} A_S & a_0^+ & \kappa^+ & \bar{D}_0^0 \\ a_0^- & B_S & \kappa^0 & \bar{D}_0^- \\ \kappa^- & \bar{\kappa}^0 & C_S & D_{s0}^- \\ D_0^0 & D_0^+ & D_{s0}^+ & D_S \end{pmatrix}, \quad T_a \pi_a = \frac{1}{\sqrt{2}} \begin{pmatrix} A_P & \pi^+ & K^+ & \bar{D}^0 \\ \pi^- & B_P & K^- & \bar{D}^- \\ K^- & \bar{K}^0 & C_P & D_s^- \\ D^0 & D^+ & D_s^+ & D_P \end{pmatrix}, \quad (B3)$$

where the diagonal elements are given as

$$\begin{aligned} A_S &= \frac{1}{2}\sigma_0 + \frac{1}{\sqrt{2}}a_0^0 + \frac{1}{\sqrt{6}}\sigma_8 + \frac{1}{\sqrt{12}}\sigma_{15}, & A_P &= \frac{1}{2}\pi_0 + \frac{1}{\sqrt{2}}\pi^0 + \frac{1}{\sqrt{6}}\pi_8 + \frac{1}{\sqrt{12}}\pi_{15}, \\ B_S &= \frac{1}{2}\sigma_0 - \frac{1}{\sqrt{2}}a_0^0 + \frac{1}{\sqrt{6}}\sigma_8 + \frac{1}{\sqrt{12}}\sigma_{15}, & B_P &= \frac{1}{2}\pi_0 - \frac{1}{\sqrt{2}}\pi^0 + \frac{1}{\sqrt{6}}\pi_8 + \frac{1}{\sqrt{12}}\pi_{15}, \\ C_S &= \frac{1}{2}\sigma_0 - \frac{2}{\sqrt{6}}\sigma_8 + \frac{1}{\sqrt{12}}\sigma_{15}, & C_P &= \frac{1}{2}\pi_0 - \frac{2}{\sqrt{6}}\pi_8 + \frac{1}{\sqrt{12}}\pi_{15}, \\ D_S &= \frac{1}{2}\sigma_0 - \frac{3}{\sqrt{12}}\sigma_{15}, & D_P &= \frac{1}{2}\pi_0 - \frac{3}{\sqrt{12}}\pi_{15}. \end{aligned} \quad (B4)$$

The nondiagonal pseudoscalar elements are defined as:

$$\begin{aligned} D^0 &= \frac{1}{\sqrt{2}}(\pi_9 + i\pi_{10}), \\ \bar{D}^0 &= \frac{1}{\sqrt{2}}(\pi_9 - i\pi_{10}), \\ D^\pm &= \frac{1}{\sqrt{2}}(\pi_{11} \pm i\pi_{12}), \\ D_s^\pm &= \frac{1}{\sqrt{2}}(\pi_{13} \pm i\pi_{14}). \end{aligned} \quad (B5)$$

The nondiagonal scalar mesons are represented as

$$\begin{aligned} D_0^0 &= \frac{1}{\sqrt{2}}(\sigma_9 + i\sigma_{10}), \\ \bar{D}_0^0 &= \frac{1}{\sqrt{2}}(\sigma_9 - i\sigma_{10}), \\ D_0^\pm &= \frac{1}{\sqrt{2}}(\sigma_{11} \pm i\sigma_{12}), \\ D_{s0}^\pm &= \frac{1}{\sqrt{2}}(\sigma_{13} \pm i\sigma_{14}). \end{aligned} \quad (B6)$$

The  $\pi_0, \pi_8$  and  $\pi_{15}$  fields are admixtures of the  $\eta, \eta', \eta_c$  mesons and the scalar fields  $\sigma_0, \sigma_8$  and  $\sigma_{15}$  are admixtures of the  $\sigma, f_0$  and  $\chi_{c0}$  mesons. In SU(4) eLSM, the interpretation of mixing pattern is assumed to be similar to that of its SU(3) configuration. Accordingly, the isoscalar states in the 15-plet -singlet  $(\eta_0, \eta_8, \eta_{15})$  are defined as

$$\begin{aligned} |\eta_0\rangle &= \frac{1}{2}(|u\bar{u}\rangle + |d\bar{d}\rangle + |s\bar{s}\rangle + |c\bar{c}\rangle), \\ |\eta_8\rangle &= \frac{1}{\sqrt{6}}(|u\bar{u}\rangle + |d\bar{d}\rangle - 2|s\bar{s}\rangle), \\ |\eta_{15}\rangle &= \frac{1}{\sqrt{12}}(|u\bar{u}\rangle + |d\bar{d}\rangle + |s\bar{s}\rangle - 3|c\bar{c}\rangle). \end{aligned} \quad (B7)$$

Defining the eigenstates for the nonstrange-strange-charm basis as  $\eta_N = (|u\bar{u}\rangle + |d\bar{d}\rangle)/\sqrt{2}$ ,  $\eta_S = |s\bar{s}\rangle$ ,  $\eta_{NS} = |c\bar{c}\rangle$ , the transition matrix can be written as:

$$\begin{pmatrix} \eta_N \\ \eta_S \\ \eta_C \end{pmatrix} = \begin{pmatrix} \frac{1}{\sqrt{2}} & \frac{1}{\sqrt{3}} & \frac{1}{\sqrt{6}} \\ \frac{1}{2} & -\sqrt{\frac{2}{3}} & \frac{1}{2\sqrt{3}} \\ \frac{1}{2} & 0 & -\frac{\sqrt{3}}{2} \end{pmatrix} \begin{pmatrix} \eta_0 \\ \eta_8 \\ \eta_{15} \end{pmatrix}. \quad (B8)$$

It should be noted that the state  $\eta_{15}$  can be identified the charmonium state  $\eta_c(1S)$  [65–67]. Because of the heavy mass of the charm quark, it is assumed to decouple almost completely from the light quarks. This means that the off-diagonal elements  $\eta_8\eta_{15}$  and  $\eta_0\eta_{15}$  become relatively small relative to  $\eta_{15}\eta_{15}$  and can be neglected also due to the mixing angles  $\theta_{015}$  and  $\theta_{815}$  are small [65, 67, 68]. Then the full  $3 \times 3$  mixing matrix can be considered as block-diagonal, specifically, a  $2 \times 2$  block for the light  $\eta/\eta'$  system and a  $1 \times 1$  block for the heavy  $\eta_c$  [67]. The physical particles are realized as  $|\eta\rangle \approx \cos\theta_P|\eta_8\rangle - \sin\theta_P|\eta_0\rangle$ ,  $|\eta'\rangle \approx \sin\theta_P|\eta_8\rangle + \cos\theta_P|\eta_0\rangle$ , where the mixing angle  $\theta_P$  is experimentally found to be about  $-41^\circ$  [69, 70]. Using the basis in Eq. (B8), the mass elements for  $\eta$  mesons can be written as [52].

$$m_{\eta'/\eta}^2 = \frac{1}{2} \left( m_N^2 + m_S^2 \pm \sqrt{(m_N^2 - m_S^2)^2 - 4m_{NS}^4} \right). \quad (B9)$$

For the scalar sector, considering the light sector only (ignoring charm completely), the mixing among the three relevant states can be parametrized in the same way as discussed above with

corresponding replacements  $(\sigma_0, \sigma_8)$ ,  $(\sigma_N, \sigma_S)$  and the scalar mixing angle  $\theta_S$  [52]. The vector  $V^\mu$  and the axial-vector  $A^\mu$  sectors are described by the following matrices:

$$V^\mu = \frac{1}{\sqrt{2}} \begin{pmatrix} \frac{1}{\sqrt{2}}(\omega_N + \rho^0) & \rho^+ & K^{*+} & D^{*0} \\ \rho^- & \frac{1}{\sqrt{2}}(\omega_N - \rho^0) & K^{*0} & D^{*-} \\ K^{*-} & \bar{K}^{*0} & \omega_S & D_s^{*-} \\ \bar{D}^{*0} & D^{*+} & D_s^{*+} & J/\psi \end{pmatrix} \quad (\text{B10})$$

$$A^\mu = \frac{1}{\sqrt{2}} \begin{pmatrix} \frac{1}{\sqrt{2}}(f_{1,N} + a_1^0) & a_1^+ & K_1^+ & \bar{D}_1^0 \\ a_1^- & \frac{1}{\sqrt{2}}(f_{1,N} - a_1^0) & K_1^0 & D_1^- \\ K_1^- & \bar{K}_1^0 & f_{1S} & D_{s1}^- \\ \bar{D}_1^0 & D_1^+ & D_{s1}^+ & \chi_{c1} \end{pmatrix}. \quad (\text{B11})$$

The missing between strange and non-strange isoscalars is neglected here [70, 71].

The mass expressions obtained for the listed states are presented in Tables A1 - A3 below. As it was said above, we express all meson masses in term of the strange–non-strange–(charm) basises.

Scalar mesons	Pseudoscalar mesons
$m_{a_0}^2 = m_0^2 + \frac{c}{\sqrt{6}}\sigma_y + \left(\lambda_1 + \frac{3}{2}\lambda_2\right)\sigma_x^2 + \lambda_1\sigma_y$ , $m_{K_0^*}^2 = Z_{K_0^*}^2$ $\times \left(m_0^2 + \frac{c}{\sqrt{2}}\sigma_y + \left(\lambda_1 + \frac{1}{2}\lambda_2\right)\sigma_x^2 + \frac{\lambda_2}{\sqrt{2}}\sigma_x\sigma_y + (\lambda_1 + \lambda_2)\sigma_y^2\right)$ , $m_{\sigma_N}^2 = m_0^2 - \frac{c\sigma_y}{\sqrt{2}} + \frac{3}{2}(2\lambda_1 + \lambda_2)\sigma_x^2 + \lambda_1\sigma_y^2$ , $m_{\sigma_S}^2 = m_0^2 + 3(\lambda_1 + \lambda_2)\sigma_y^2 + \lambda_1\sigma_x^2$ , $m_{\sigma_{SN}}^2 = -\frac{c\sigma_x}{\sqrt{2}} + 2\lambda_1\sigma_x\sigma_y$ .	$m_\pi^2 = Z_\pi^2 \left(m_0^2 - \frac{c}{\sqrt{2}}\sigma_y + \left(\lambda_1 + \frac{\lambda_2}{2}\right)\sigma_x^2 + \lambda_1\sigma_y^2\right)$ , $m_K^2 = Z_K^2$ $\times \left(m_0^2 - \frac{c}{2}\sigma_x + \left(\lambda_1 + \frac{\lambda_2}{2}\right)\sigma_x^2 + (\lambda_1 + \lambda_2)\sigma_y^2 - \frac{\lambda_2}{\sqrt{2}}\sigma_x\sigma_y\right)$ , $m_{\eta_N}^2 = Z_\pi^2 \left(m_0^2 + \frac{c}{\sqrt{2}}\sigma_y + \left(\lambda_1 + \frac{\lambda_2}{2}\right)\sigma_x^2 + \lambda_1\sigma_y^2\right)$ , $m_{\eta_S}^2 = Z_{\eta_S}^2 \left(m_0^2 + \lambda_1\sigma_x^2 + (\lambda_1 + \lambda_2)\sigma_y^2\right)$ , $m_{\eta_{NS}}^2 = Z_\pi^2 Z_{\eta_S}^2 \frac{c}{2}\sigma_x$ .
Vector mesons	Axial-vector mesons
$m_\rho^2 = m_1^2 + \frac{h_1}{2}(\sigma_x^2 + \sigma_y^2) + \frac{1}{2}(h_2 + h_3)\sigma_x^2 + 2\delta_x$ , $m_{K^*}^2 = m_1^2 + \frac{h_1}{2}(\sigma_x^2 + \sigma_y^2) + \frac{1}{4}(g_1^2 + h_2)(\sigma_x^2 + 2\sigma_y^2)$ $+ \frac{\sigma_x\sigma_y}{\sqrt{2}}(h_3 - g_1^2) + \delta_x + \delta_y$ , $m_{\omega_S}^2 = m_1^2 + \frac{h_1}{2}(\sigma_x^2 + \sigma_y^2) + (h_2 + h_3)\sigma_y^2 + 2\delta_y$ , $m_{\omega_N}^2 = m_\rho^2$ .	$m_{a_1}^2 = m_1^2 + g_1^2\sigma_x^2 + \frac{h_1}{2}(\sigma_x^2 + \sigma_y^2) + \frac{1}{2}(h_2 - h_3)\sigma_x^2 + 2\delta_x$ , $m_{K_1}^2 = m_1^2 + \frac{h_1}{2}(\sigma_x^2 + \sigma_y^2) + \frac{1}{4}(g_1^2 + h_2)(\sigma_x^2 + 2\sigma_y^2)$ $- \frac{\sigma_x\sigma_y}{\sqrt{2}}(h_3 - g_1^2) + \delta_x + \delta_y$ , $m_{f_{1S}}^2 = m_1^2 + 2g_1^2\sigma_y^2 + \frac{h_1}{2}(\sigma_x^2 + \sigma_y^2) + (h_2 - h_3)\sigma_y^2 + 2\delta_y$ , $m_{f_{1N}}^2 = m_{a_1}^2$ .

**Tab. A1.** The meson masses for SU(3) configuration

Scalar non-charmed mesons	Pseudoscalar non-charmed mesons
$m_{a_0}^2 = m_0^2 + \frac{c}{2} \sigma_c \sigma_y + \lambda_1 (\sigma_x^2 + \sigma_y^2 + \sigma_c^2) + \frac{3\lambda_2}{2} \sigma_x^2,$ $m_{K_0^*}^2 = Z_{K_0^*}^2 \left( m_0^2 + \frac{c}{2\sqrt{2}} \sigma_x \sigma_c + \left( \lambda_1 + \frac{\lambda_2}{2} \right) \sigma_x^2 + \lambda_1 (\sigma_y^2 + \sigma_c^2) + \frac{\lambda_2}{\sqrt{2}} \sigma_x \sigma_y + \lambda_2 \sigma_y^2 \right),$ $m_{\sigma_N}^2 = m_0^2 - \frac{c}{2} \sigma_c \sigma_y + 3 \left( \lambda_1 + \frac{\lambda_2}{2} \right) \sigma_x^2 + \lambda_1 (\sigma_y^2 + \sigma_c^2)$ $m_{\sigma_S}^2 = m_0^2 + \lambda_1 (\sigma_x^2 + \sigma_c^2) + 3 (\lambda_1 + \lambda_2) \sigma_y^2,$ $m_{\sigma_{NS}}^2 = 2 \lambda_1 \sigma_x \sigma_y - \frac{c}{2} \sigma_c \sigma_x.$	$m_{\pi}^2 = Z_{\pi}^2 \left( m_0^2 - \frac{c}{2} \sigma_y \sigma_c + \left( \lambda_1 + \frac{\lambda_2}{2} \right) \sigma_x^2 + \lambda_1 \sigma_y^2 + \lambda_1 \sigma_c^2 \right),$ $m_K^2 = Z_K^2 \left( m_0^2 - \frac{c}{2\sqrt{2}} \sigma_x \sigma_c + \left( \lambda_1 + \frac{\lambda_2}{2} \right) \sigma_x^2 + \lambda_1 (\sigma_y^2 + \sigma_c^2) - \frac{\lambda_2}{\sqrt{2}} \sigma_x \sigma_y + \lambda_2 \sigma_y^2 \right),$ $m_{\eta_N}^2 = Z_{\eta_N}^2 \left( m_0^2 + \frac{c}{2} \sigma_c \sigma_y + \left( \lambda_1 + \frac{\lambda_2}{2} \right) \sigma_x^2 + \lambda_1 (\sigma_y^2 + \sigma_c^2) \right),$ $m_{\eta_S}^2 = Z_{\eta_S}^2 \left( m_0^2 + \lambda_1 (\sigma_x^2 + \sigma_c^2) + (\lambda_1 + \lambda_2) \sigma_y^2 \right),$ $m_{\eta_{NS}}^2 = -Z_{\pi} Z_{\eta_S} \frac{c}{2} \sigma_x \sigma_c.$
Vector non-charmed mesons	Axial-vector non-charmed mesons
$m_{\rho}^2 = m_1^2 + \frac{h_1}{2} (\sigma_x^2 + \sigma_y^2 + \sigma_c^2) + \frac{1}{2} (h_2 + h_3) \sigma_x^2 + 2\delta_x,$ $m_{K^*}^2 = m_1^2 + \frac{h_1}{2} (\sigma_x^2 + \sigma_y^2 + \sigma_c^2) + \frac{1}{4} (g_1^2 + h_2) (\sigma_x^2 + 2\sigma_y^2) + \frac{\sigma_x \sigma_y}{\sqrt{2}} (h_3 - g_1^2) + \delta_x + \delta_y,$ $m_{\omega_S}^2 = m_1^2 + \frac{h_1}{2} (\sigma_x^2 + \sigma_y^2 + \sigma_c^2) + (h_2 + h_3) \sigma_y^2 + 2\delta_y,$ $m_{\omega_N}^2 = m_{\rho}^2.$	$m_{a_1}^2 = m_1^2 + g_1^2 \sigma_x^2 + \frac{h_1}{2} (\sigma_x^2 + \sigma_y^2 + \sigma_c^2) + \frac{1}{2} (h_2 - h_3) \sigma_x^2 + 2\delta_x,$ $m_{K_1}^2 = m_1^2 + \frac{h_1}{2} (\sigma_x^2 + \sigma_y^2 + \sigma_c^2) + \frac{1}{4} (g_1^2 + h_2) (\sigma_x^2 + 2\sigma_y^2) - \frac{\sigma_x \sigma_y}{\sqrt{2}} (h_3 - g_1^2) + \delta_x + \delta_y,$ $m_{f_{1S}}^2 = m_1^2 + 2g_1^2 \sigma_y^2 + \frac{h_1}{2} (\sigma_x^2 + \sigma_y^2 + \sigma_c^2) + (h_2 - h_3) \sigma_y^2 + 2\delta_y,$ $m_{f_{1N}}^2 = m_{a_1}^2.$

**Tab. A2.** The non-charmed meson masses for SU(4) configuration.

Scalar charmed mesons	Pseudoscalar charmed mesons
$m_{\chi_{c0}}^2 = m_0^2 + \lambda_1 (\sigma_x^2 + \sigma_y^2) + 3 (\lambda_1 + \lambda_2) \sigma_c^2 + 2\epsilon_c,$ $m_{D_0^*}^2 = Z_{D_0^*}^2 \left( m_0^2 - \frac{c}{2\sqrt{2}} \sigma_x \sigma_y + \left( \lambda_1 + \frac{\lambda_2}{2} \right) \sigma_x^2 + \lambda_1 \sigma_y^2 + (\lambda_1 + \lambda_2) \sigma_c^2 + \frac{\lambda_2}{\sqrt{2}} \sigma_x \sigma_c + \epsilon_c \right),$ $m_{D_{s0}^*}^2 = Z_{D_{s0}^*}^2 \left( m_0^2 - \frac{c}{4} \sigma_x^2 + \lambda_1 \sigma_x^2 + (\lambda_1 + \lambda_2) \sigma_y^2 + \lambda_2 \sigma_y \sigma_c + (\lambda_1 + \lambda_2) \sigma_c^2 + \epsilon_c \right)$	$m_D^2 = Z_D^2 \left( m_0^2 + \frac{c}{2\sqrt{2}} \sigma_x \sigma_y + \left( \lambda_1 + \frac{\lambda_2}{2} \right) \sigma_x^2 + \lambda_1 \sigma_y^2 + (\lambda_1 + \lambda_2) \sigma_c^2 - \frac{\lambda_2}{\sqrt{2}} \sigma_x \sigma_c + \epsilon_c \right),$ $m_{\eta_c}^2 = Z_{\eta_c}^2 \left( m_0^2 + \lambda_1 (\sigma_x^2 + \sigma_y^2) + (\lambda_1 + \lambda_2) \sigma_c^2 + 2\epsilon_c \right),$ $m_{D_s}^2 = Z_{D_s}^2 \left( m_0^2 + \frac{c}{4} \sigma_x^2 + \lambda_1 \sigma_x^2 + (\lambda_1 + \lambda_2) \sigma_y^2 + (\lambda_1 + \lambda_2) \sigma_c^2 - \lambda_2 \sigma_y \sigma_c + \epsilon_c \right).$
Vector charmed mesons	Axial-vector charmed mesons
$m_{D^*}^2 = m_1^2 + \frac{h_1}{2} (\sigma_x^2 + \sigma_y^2 + \sigma_c^2) + \frac{1}{4} (g_1^2 + h_2) (\sigma_x^2 + 2\sigma_c^2) + \frac{\sigma_x \sigma_c}{\sqrt{2}} (h_3 - g_1^2) + \delta_x + \delta_c,$ $m_{J/\psi}^2 = m_1^2 + \frac{h_1}{2} (\sigma_x^2 + \sigma_y^2 + \sigma_c^2) + (h_2 + h_3) \sigma_c^2 + 2\delta_c,$ $m_{D_s^*}^2 = m_1^2 + \frac{h_1}{2} (\sigma_x^2 + \sigma_y^2 + \sigma_c^2) + \frac{1}{2} (g_1^2 + h_2) (\sigma_y^2 + \sigma_c^2) + (h_3 - g_1^2) \sigma_y \sigma_c + \delta_y + \delta_c.$	$m_{D_1}^2 = m_1^2 + \frac{h_1}{2} (\sigma_x^2 + \sigma_y^2 + \sigma_c^2) + \frac{1}{4} (g_1^2 + h_2) (\sigma_x^2 + 2\sigma_c^2) + \frac{\sigma_x \sigma_c}{\sqrt{2}} (g_1^2 - h_3) + \delta_x + \delta_c,$ $m_{\chi_{c1}}^2 = m_1^2 + 2g_1^2 \sigma_c^2 + \frac{h_1}{2} (\sigma_x^2 + \sigma_y^2 + \sigma_c^2) + (h_2 - h_3) \sigma_c^2 + 2\delta_c,$ $m_{D_{s1}}^2 = m_1^2 + \frac{h_1}{2} (\sigma_x^2 + \sigma_y^2 + \sigma_c^2) + \frac{1}{2} (g_1^2 + h_2) (\sigma_y^2 + \sigma_c^2) + \sigma_y \sigma_c (g_1^2 - h_3) + \delta_y + \delta_c,$

**Tab. A3.** The masses of mesons with open (hidden) charm.

### C. Derivations of Squared Quark Mass

In Section II C, it was noted that the in-medium meson masses are influenced by the quark contribution, Eq. (32). The results for the first and second derivatives of the quark mass with respect to the meson fields for the SU(3) configuration can be found for example in Refs. [52, 59]. Our results for SU(4) configuration are presented in Tab. A4. The degenerate light flavours are presented in second and third,  $m_{f,a}^2 m_{f,b}^2/g^4$ ,  $m_{f,ab}^2/g^2$ , the strange quark in fourth and fifth,  $m_{y,a}^2 m_{y,b}^2/g^4$ ,  $m_{y,ab}^2/g^2$ , and the charm quark in last two columns,  $m_{c,a}^2 m_{c,b}^2/g^4$ ,  $m_{c,ab}^2/g^2$ .

	$m_{f,a}^2 m_{f,b}^2/g^4$	$m_{f,ab}^2/g^2$	$m_{y,a}^2 m_{y,b}^2/g^4$	$m_{y,ab}^2/g^2$	$m_{c,a}^2 m_{c,b}^2/g^4$	$m_{c,ab}^2/g^2$
$\sigma_0 \sigma_0$	$\frac{1}{4}\sigma_x^2$	$\frac{1}{2}$	$\frac{1}{4}\sigma_y^2$	$\frac{1}{4}$	$\frac{1}{4}\sigma_c^2$	$\frac{1}{4}$
$\sigma_1 \sigma_1$	0	1	0	0	0	0
$\sigma_4 \sigma_4$	0	$\sigma_x \frac{\sigma_x + \sqrt{2}\sigma_y}{\sigma_x^2 - 2\sigma_y^2}$	0	$\sigma_y \frac{\sqrt{2}\sigma_x + 2\sigma_y}{\sigma_x^2 - 2\sigma_y^2}$	0	0
$\sigma_7 \sigma_7$	0	$\frac{1}{2}$	0	$\frac{1}{2}$	0	0
$\sigma_9 \sigma_9$	0	$\frac{1}{2}$	0	0	0	$\frac{1}{2}$
$\sigma_{11} \sigma_{11}$	0	$\frac{1}{2}$	0	0	0	$\frac{1}{2}$
$\sigma_{13} \sigma_{13}$	0	0	0	$\frac{1}{2}$	0	$\frac{1}{2}$
$\sigma_{15} \sigma_{15}$	$\frac{1}{12}\sigma_x^2$	$\frac{1}{6}$	$\frac{1}{12}\sigma_y^2$	$\frac{1}{12}$	$\frac{3}{4}\sigma_c^2$	$\frac{3}{4}$
$\sigma_8 \sigma_8$	$\frac{1}{6}\sigma_x^2$	$\frac{1}{3}$	$\frac{2}{3}\sigma_y^2$	$\frac{2}{3}$	0	0
$\sigma_0 \sigma_8$	$\frac{1}{2\sqrt{6}}\sigma_x^2$	$\frac{1}{\sqrt{6}}$	$\frac{1}{\sqrt{6}}\sigma_y^2$	$-\frac{1}{\sqrt{6}}$	0	0
$\sigma_0 \sigma_{15}$	$\frac{1}{4\sqrt{3}}\sigma_x^2$	$\frac{1}{2\sqrt{3}}$	$\frac{1}{4\sqrt{3}}\sigma_y^2$	$\frac{1}{4\sqrt{3}}$	$-\frac{\sqrt{3}}{4}\sigma_c^2$	$-\frac{\sqrt{3}}{4}$
$\sigma_8 \sigma_{15}$	$\frac{1}{6\sqrt{2}}\sigma_x^2$	$-\frac{1}{3\sqrt{2}}$	$\frac{1}{3\sqrt{2}}\sigma_y^2$	$-\frac{1}{3\sqrt{2}}$	0	0
$\pi_0 \pi_0$	0	$\frac{1}{2}$	0	$\frac{1}{4}$	0	$\frac{1}{4}$
$\pi_1 \pi_1$	0	1	0	0	0	0
$\pi_4 \pi_4$	0	$\sigma_x \frac{\sigma_x - \sqrt{2}\sigma_y}{\sigma_x^2 - 2\sigma_y^2}$	0	$\sigma_y \frac{\sqrt{2}\sigma_x - 2\sigma_y}{\sigma_x^2 - 2\sigma_y^2}$	0	0
$\pi_7 \pi_7$	0	$\frac{1}{2}$	0	$\frac{1}{2}$	0	0
$\pi_9 \pi_9$	0	$\frac{1}{2}$	0	0	0	$\frac{1}{2}$
$\pi_{11} \pi_{11}$	0	$\frac{1}{2}$	0	0	0	$\frac{1}{2}$
$\pi_{13} \pi_{13}$	0	0	0	$\frac{1}{2}$	0	$\frac{1}{2}$
$\pi_{15} \pi_{15}$	0	$\frac{1}{6}$	0	$\frac{1}{12}$	0	$\frac{3}{4}$
$\pi_8 \pi_8$	0	$\frac{1}{3}$	0	$\frac{2}{3}$	0	0
$\pi_0 \pi_8$	0	$\frac{1}{\sqrt{6}}$	0	$-\frac{1}{\sqrt{6}}$	0	0
$\pi_0 \pi_{15}$	0	$\frac{1}{2\sqrt{3}}$	0	$\frac{1}{4\sqrt{3}}$	0	$-\frac{\sqrt{3}}{4}$
$\pi_8 \pi_{15}$	0	$\frac{1}{3\sqrt{2}}$	0	$-\frac{1}{3\sqrt{2}}$	0	0

**Tab. A4.** First and second derivatives of the squared quark mass with respect to the meson fields.